Nicholson, K.N., and Abu El-Rus, M.A., 2022, A case of Ampferer-type subduction beneath the New Caledonia arc: Evidence for inefficient subduction of hydrated lithologies into the upper mantle: GSA Bulletin, https://doi.org/10.1130/B36166.1.

Supplemental Material

Figure S1. Main petrographic features of the La Conception lava.

Figure S2. Major and trace elements abundance of the melt fractions resulting from reverse fractionation modeling for Sample NC-01as an example of La Conception lavas.

Figure S3. Primitive-mantle normalized patterns of melt fractions resulting from reverse fractionation modeling of samples NC-01 and NC-05 under oxidizing (fO_2 buffered Fe_3 + /ΣFe = 0.32); and (*f*O2 buffered Fe3+/ΣFe = 0.18), respectively.

Figure S4. Plots showing the conservative behavior of the incompatible trace element ratios during fractional crystallization of Samples NC-01 and NC-05.

Figure S5. Bivariate proxy plots illustrating the conservative and non-conservator elements in the La Conception Lava. N-MORB, D-MORB (La/SmN < 0.8) and E-MORB (La/SmN > 1.5) are respectively the log-normal mean, weighted by segment length of the normal MORB, depleted MORB and enriched MORB, respectively.

Table S1. Partition coefficient values used for estimation abundance of the trace elements

Table S2. Primary melt compositions calculated to Mg# ~ 072 and their intensive parameters as estimated by Petrolog software version 3.1.1.3. Norm compositions (wt%) are shown.

Table S3. The percentage of the subduction component (%sz) of the elements in the La Conception estimated from the displacement from the average MORB at given Nb.

Table S4. Trace element abundances (ppm) of the primitive mantle (after McDonough and Sun, 1995).

Table S5. Mineral/mineral partition coefficients used in the modeling of melting mantle peridotite.

Table S6. Mineral proportions in the initial source.

Table S7. Intensive and extensive melting parameters calculating from the composition of the La Conception lavas assuming 0 wt% of their pre-eruptive H_2O content.

Table S8. Intensive and extensive melting parameters calculating from the composition of the La Conception lavas assuming 4 wt% of their pre-eruptive H_2O content.

Table S9. Intensive and extensive melting parameters calculating from the composition of the La Conception lavas assuming 8 wt% of their pre-eruptive H_2O content.

Appendix A

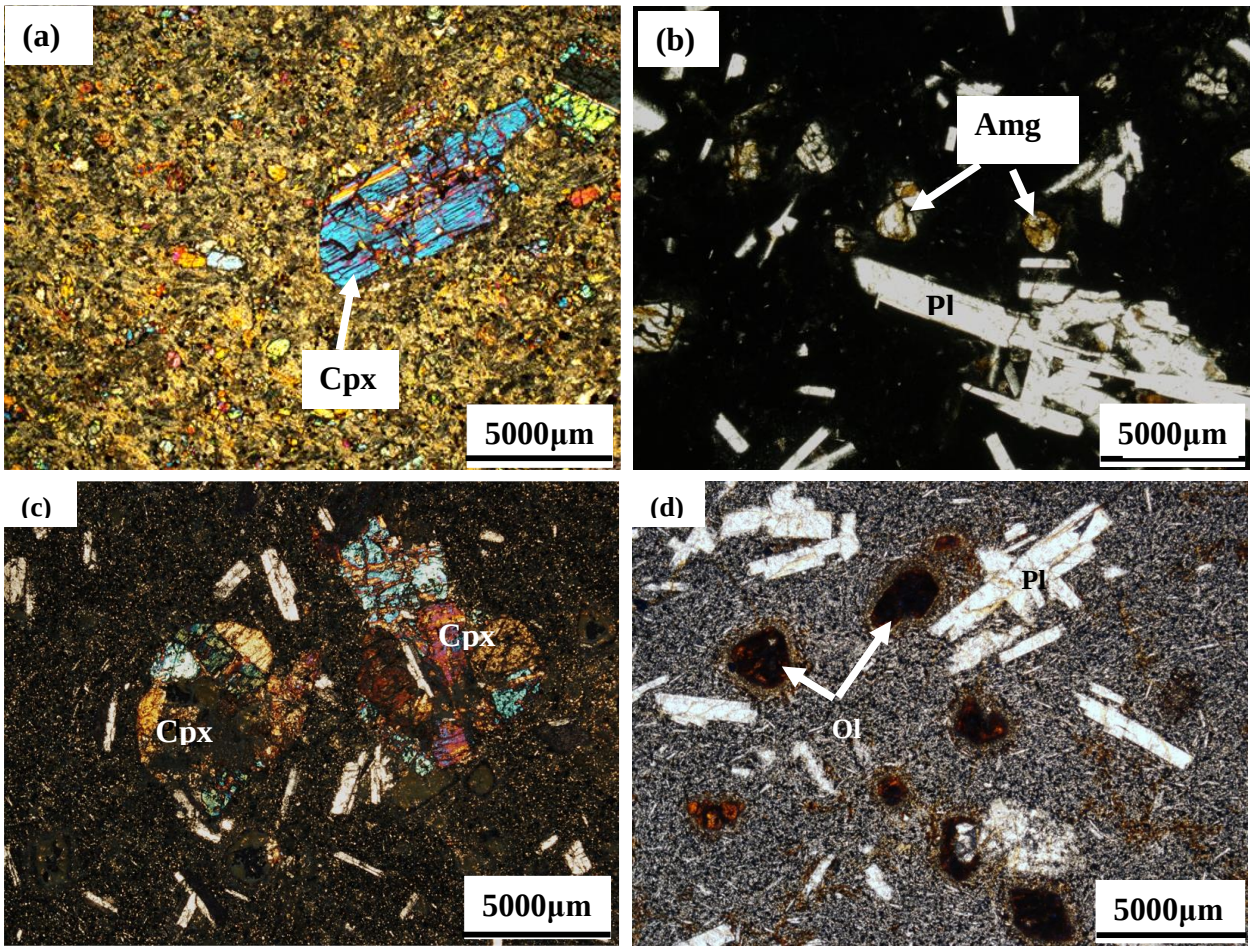

(Fig A1): Main petrographic features of the La Conception lava: (a) Clinopyroxene (cpx) micro-phenocryst set in the devitrified groundmass. Note the disequilibrium outlines exhibited by cpx crystal against the groundmass; (b) Euhedral plagioclase (pl) micro-phenocryst set in the glassy groundmass. Note that the groundmass contains minute round amygdales (Amg) filled with chlorite (white) and calcite (brown); (c) Well-rounded aggregate of clinopyroxene micro-phenocrysts and subhedral to euhedral plagioclase set in the hypohyaline groundmass.; (d) Subhedral to euhedral plagioclase laths and rounded blebs of olivine crystals, totally altered to reddish-brown iddingsite.

Appendix B

Conditions used in the running Petrolog 3.1.1.3 program.

a. Models used for estimating the abundance of major elements.

For olivine-melt, and clinopyroxene-melt equilibria, the model of Weaver & Langmuir (1990) is used and for Cr-spinel-melt equilibrium, the model of Ariskin and Nikolaev (1996) is used. Melt density, viscosity and oxidation state are calculated from formulations of Lange and Carmichael (1987), Bottinga, and Weill, (1972) and Borisov and Shapkin (1990), respectively.

Table (I) Partition coefficient values used for estimation abundance of the trace elements

Element	Ol	Cpx	Cr-sp
Sc	0.25	2.28	0.24
V	0.09	0.6	15
Co	5.21	0.95	5
Ni	22.28	2.84	10
Rb	0.00032	0.0047	1.00E-08
Sr	0.0005	0.1283	0.0001
Y	0.0131	0.492	0.0004
Zr	0.00068	0.123	0.005
Nb	5.00E-05	0.05	0.001
Cs	0.00032	0.001	1.00E-08
Ba	0.00032	0.00068	1.00E-08
La	3.10E-05	0.0536	0.0004
Ce	0.0001	0.0858	0.0005
Pr	0.00027*	0.13655*	0.00065
Nd	0.00042	0.1873	0.00058
Sm	0.0011	0.291	0.00048
Eu	0.00075	0.3288*	0.00045
Gd	0.0012	0.3665*	0.00042
Tb	0.0013*	0.4043*	0.00041
Dy	0.0014	0.442	0.0004
Ho	0.0072*	0.415*	0.00041
Er	0.013	0.387	0.00042

Tm	0.0215*	0.4085*	0.00045
Yb	0.03	0.43	0.00048
Lu	0.039	0.423	0.00053
Hf	0.0011	0.256	0.01
Ta	5.00E-05	0.019	0.002
Pb	0.0001	0.072	0.0007
Th	5.20E-05	0.012	1.00E-08
U	2.00E-05	0.0103	1.00E-08

For olivine Sc, V, Co, Ni, Sr and Y are from Laubier *et al.* (2014); other trace elements except for Cs, Rb, Ta and Pb are from Kennedy *et al*. (1993). Unavailable partition coefficient values of Cs, Rb, Ta and Nb are set equal to the values of their neighbors in the compatibility arrangement: Cs and Rb equal to Ba; Ta equal to Nb and Pb equal to Ce.

For clinopyroxene Sc, V, Co, Ni, Sr, Y, Zr, Nb are from Laubier *et al*. (2014); Cs, Rb, Ta, Th and U are from Zack *et al.* (1997); other trace elements are from Hart and Dunn (1993).

For spinel, V, Co, Ni data determined by Righter *et al*. (2006) for fractionation komatiites, MORB and Hawaiian OIB that are evolved near the QFM buffer; Sc is from Horn *et al*. (1994); other elements are from compilation of Ionov *et al.* (2002). Unavailable partition coefficient values of Cs, Rb, Ba and Y are set equal to the values of their neighbors in the compatibility arrangement: Cs, Rb and Ba equal to Th; Y equal to Dy.

* interpolated values.

b. Table (AII) Primary melt compositions calculated to Mg# ~ 072 and their intensive parameters as estimated by Petrolog software version 3.1.1.3. Norm compositions (wt.%) are shown.

Samples	NC-00		NC-01		NC-02		NC-03		NC-04		NC-05		NC-06	
Run	Fe^{3+}/∑Fe 0.32	Fe^{3+}/∑Fe 018	Fe^{3+}/∑Fe 0.32	Fe^{3+}/∑Fe 018	Fe^{3+}/∑Fe 0.32	Fe^{3+}/∑Fe 018	Fe^{3+}/∑Fe 0.32	Fe^{3+}/∑Fe 018	Fe^{3+}/∑Fe 0.32	Fe^{3+}/∑Fe 018	Fe^{3+}/∑Fe 0.32	Fe^{3+}/∑Fe 018	Fe^{3+}/∑Fe 0.32	Fe^{3+}/∑Fe 018
Major oxides (wt%)														
SiO_2	53.64	53.67	56.56	56.49	55.51	55.5	54.84	54.85	56.1	55.97	54.77	54.57	54.29	54.35
TiO_2	0.69	0.65	0.69	0.66	0.69	0.66	0.71	0.68	0.7	0.66	0.68	0.63	0.74	0.69
Al_2O_3	11.31	10.46	11.18	10.55	11.41	10.87	11.48	10.79	11.63	10.74	11.09	10.57	12.12	11.19
Fe_2O_3	3.05	1.92	2.72	1.54	2.62	1.62	2.58	1.51	2.57	1.55	3.23	2.12	2.78	1.51
FeO	6.33	6.89	6.55	7.37	6.38	7.08	6.43	7.1	5.9	6.49	6.16	6.62	6.32	7.09
MnO	0.12	0.1	0.12	0.11	0.12	0.12	0.12	0.11	0.11	0.1	0.12	0.12	0.13	0.11
MgO	9.1	9.87	9.5	10.65	9.28	10.13	9.34	10.3	8.51	9.65	8.93	9.28	9.03	10.31
CaO	11.38	12.4	7.05	7.36	7.6	7.99	8.36	8.93	8.2	9.08	11.28	12.26	8.19	8.86
Na_2O	1.95	1.78	2.08	1.95	2.65	2.51	2.59	2.42	3.3	3.02	2.71	2.67	2.68	2.45
K_2O	1.67	1.52	2.75	2.55	2.9	2.73	2.77	2.57	2.28	2.07	0.45	0.38	2.93	2.65
P_2O_5	0.47	0.43	0.49	0.46	0.48	0.45	0.47	0.44	0.44	0.4	0.25	0.2	0.49	0.44
Cr_2O_3	0.06	0.09	0.03	0.05	0.03	0.05	0.04	0.06	0.03	0.05	0.06	0.1	0.03	0.05
Total	99.77	99.78	99.72	99.74	99.67	99.71	99.73	99.76	99.77	99.78	99.73	99.52	99.73	99.7
Trace element abundances (ppm)														
Sc	47.3	53.5	43.8	48.3	44	47.7	46	50.9	42.1	47.8	37.3	34.4	44.6	50.8
V	204.7	199.7	178.9	175	199.8	196.5	194.2	190	192.7	187.6	214.4	186.6	203.7	197.9
Co	26	26	25.7	25.7	25.9	25.9	25.2	25.2	24.1	24.1	31.8	28.5	26.6	26.6
Ni	79.9	96.4	73.6	85.1	84	94.7	83.6	97.2	62.5	75.5	151.6	155.5	94.9	115.1
Cu	63	57.2	21.2	19.7	49.4	46.4	83.8	77.5	38.5	34.9	78	65.2	25	22.6
Zn	59.9	54.4	64.8	60.1	67.5	63.4	65.6	60.7	64.2	58.2	63.2	52.8	73.3	66.4
Rb	38	34.5	83.8	77.8	564.1	530.4	76.7	71	61.4	55.7	10.1	8.4	91.7	83
Sr	723.7	665.6	850	796.5	746.8	707.7	806.5	753.7	612.3	562.3	349.7	293.9	879	805.7
Y	15.6	14.9	16.3	15.7	16.2	15.7	16.9	16.2	17.2	16.4	16	13.7	17.3	16.4
Zr	121.9	112.1	126.1	118.1	123.1	116.6	126.1	117.8	134.4	123.4	123.8	104	129.6	118.7
Nb	7.8	7.1	8.3	7.7	7.5	7.1	7.2	6.7	8.6	7.9	7.8	6.6	8.4	7.6
Ba	321	291.6	560.4	520.1	563.6	529.9	520.2	481.3	498.8	452.4	64	53.5	610.8	552.8
La	20.1	18.3	20.7	19.3	20.5	19.3	22	20.5	23.9	21.8	22.5	18.8	22.6	20.5
Ce	44.5	40.7	46.8	43.7	46.6	44.1	47.7	44.5	52.2	47.8	48.3	40.5	49.2	44.9

Nd	24	22.2	26.2	24.7	26.3	25	25.6	24	28.1	26	26.5	22.4	26.9	24.8
Sm	5.2	4.9	5.4	5.1	5.8	5.5	5.3	5	5.7	5.4	5.6	4.8	5.6	5.2
Eu	1.5	1.4	1.7	1.6	1.6	1.5	1.7	1.6	1.7	1.6	1.7	1.4	1.6	1.5
Gd	5.1	4.8	5.3	5	5	4.8	5.4	5.1	5.4	5.1	5.3	4.5	5.5	5.1
Tb	0.7	0.6	0.7	0.7	0.7	0.7	0.7	0.7	0.7	0.7	0.7	0.6	0.7	0.7
Dy	3.4	3.2	3.6	3.5	3.4	3.2	3.4	3.3	3.7	3.5	3.4	2.9	3.6	3.4
Ho	0.7	0.6	0.6	0.6	0.6	0.6	0.7	0.7	0.7	0.6	0.6	0.5	0.7	0.6
Er	1.8	1.7	2	2	1.9	1.8	2	1.9	2	1.9	1.8	1.6	1.8	1.7
Tm	0.2	0.2	0.2	0.2	0.2	0.2	0.2	0.2	0.2	0.2	0.2	0.2	0.2	0.2
Yb	1.5	1.4	1.5	1.5	1.6	1.6	1.6	1.5	1.6	1.5	1.5	1.3	1.5	1.5
Lu	0.2	0.2	0.2	0.2	0.3	0.2	0.2	0.2	0.3	0.2	0.2	0.2	0.2	0.2
Hf	3.3	3	3.5	3.3	3.5	3.3	3.4	3.2	3.6	3.3	3.6	3	3.5	3.2
Pb	8.6	7.9	6.7	6.2	8.3	7.9	8	7.5	9.5	8.7	9.6	8.1	8.4	7.7
Th	3.2	2.9	3.6	3.4	3.5	3.3	3.7	3.4	4.5	4	3.5	2.9	3.5	3.2
U	1.1	1	1.2	1.1	1.2	1.1	1.2	1.1	1.5	1.3	1.2	1	1.3	1.1
CIPW Norm														
Q	3.37	2.00	6.06	4.39	1.46	0.28	0.49		1.59	0.42	5.48			
Or	9.87	8.98	16.25	15.07	17.14	16.13	16.37	15.19	13.47	12.23	2.66	2.25	17.32	15.66
Ab	16.50	15.06	17.60	16.50	22.42	21.24	21.92	20.48	27.92	25.55	22.93	19.21	22.68	20.73
An	17.17	16.06	13.05	12.50	10.67	10.33	11.52	10.99	10.19	9.64	16.77	14.25	12.39	11.71
Di	29.12	34.40	15.07	16.96	19.23	21.29	21.64	24.57	22.22	26.44	28.73	29.74	20.15	23.71
Hy	16.90	18.21	25.30	29.74	22.53	25.78	21.61	22.22	18.31	21.06	16.23	14.73	19.28	18.82
Ol								1.79				14.86	1.35	4.54
Mt	4.42	2.78	3.94	2.23	3.80	2.35	3.74	2.19	3.73	2.25	4.68	2.90	4.03	2.19
Il	1.31	1.23	1.31	1.25	1.31	1.25	1.35	1.29	1.33	1.25	1.29	1.10	1.41	1.31
Ap	1.09	1.00	1.14	1.07	1.11	1.04	1.09	1.02	1.02	0.93	1.04	0.88	1.14	1.02
Extensive and intensive parameters														
D(g/cm^3)	2.646	2.65	2.611	2.618	2.61	2.616	2.618	2.624	2.598	2.607	2.64	2.685	2.619	2.627
V(poise)	435	505	1480	933	1200	823	931	591	1365	734	479	448	1081	602
Log(f_{O2})	-5.3	-6.3	-5.8	-6.9	-6	-7	-6	-7	-6.5	-6.9	-5.1	-6.8	-6	-7.1
Fractionation phase proportion (wt%)														
Cpx	21.90	29.07	17.98	23.94	17.98	22.94	20.97	26.92	15.00	21.927	10.45	14.05	16.99	24.92
Cr-spinel	0.10	0.17	0.02	0.06	0.02	0.07	0.04	0.09	0.01	0.075	0.09	0.18	0.02	0.08
Olivine		traces									4.47	4.78		
Melt	78.00	70.76	82.00	76.00	82.00	77.00	79.00	73.00	84.99	78	84.99	80.99	83.00	75.00

Initial composition of fractionation phases														
Mg# (cpx)	88.16	89.48	88.69	90.04	88.74	89.81	88.80	90.04	88.50	89.91	87.97	89.27	88.38	90.06
Cr#(spine)	60.8	69.64	73.49	69.36	57.08	67.15	57.56	68.81	55.55	68.49	62.34	75.61	52.89	66.44
Fo(Olivine)		88.77									86.61	88.47		

Table (II):*Continued*

Samples	NC-07		NC-08		NC-09		NC-10		NC-11		NC-12		NC-13	
Run	$Fe^{3+}/\sum Fe$ 0.32	$Fe^{3+}/\sum Fe$ 018	$Fe^{3+}/\sum Fe$ 0.32	$Fe^{3+}/\sum Fe$ 018	$Fe^{3+}/\sum Fe$ 0.32	$Fe^{3+}/\sum Fe$ 018	$Fe^{3+}/\sum Fe$ 0.32	$Fe^{3+}/\sum Fe$ 018	$Fe^{3+}/\sum Fe$ 0.32	$Fe^{3+}/\sum Fe$ 018	$Fe^{3+}/\sum Fe$ 0.32	$Fe^{3+}/\sum Fe$ 018	$Fe^{3+}/\sum Fe$ 0.32	$Fe^{3+}/\sum Fe$ 018
Major oxides (w%)														
SiO_2	54.55	54.65	54.44	54.27	56.31	56.24	56.04	55.94	53.11	53.22	55.22	55.01	57.99	57.79
TiO_2	0.75	0.72	0.72	0.68	0.71	0.68	0.7	0.67	0.72	0.68	0.71	0.68	0.66	0.63
Al_2O_3	12.34	11.67	12.39	11.58	11.44	10.8	11.47	10.72	11.87	11.16	11.65	11.06	10.81	10.21
Fe_2O_3	2.57	1.39	2.59	1.6	2.63	1.53	2.67	1.54	2.77	1.65	3.04	2.09	2.54	1.51
FeO	7.08	7.92	5.51	6.19	6.22	6.97	6.07	6.8	6.52	7.2	5.89	6.55	5.84	6.56
MnO	0.13	0.12	0.13	0.12	0.12	0.11	0.12	0.11	0.12	0.11	0.12	0.12	0.14	0.13
MgO	10.11	11.46	7.87	8.95	9.08	10.14	8.78	9.92	9.47	10.31	8.54	9.36	8.43	9.44
CaO	6.16	6.15	10.8	11.45	7.65	8.07	8.29	8.87	9.83	10.45	11.9	12.34	7.62	8.14
Na_2O	2.08	1.95	2.65	2.46	2.28	2.14	2.16	2.01	2.05	1.91	1.77	1.67	2.34	2.19
K_2O	3.47	3.22	2.19	2.01	2.77	2.57	2.88	2.64	2.69	2.49	0.41	0.39	2.85	2.65
P_2O_5	0.52	0.48	0.46	0.43	0.49	0.46	0.53	0.48	0.55	0.51	0.54	0.5	0.49	0.46
Cr_2O_3	0.03	0.04	0.04	0.06	0.03	0.05	0.03	0.05	0.04	0.07	0.06	0.08	0.03	0.04
Total	99.79	99.77	99.79	99.8	99.73	99.76	99.74	99.75	99.74	99.76	99.85	99.85	99.74	99.75
Trace element abundances (ppm)														
Sc	43.4	47.8	37.3	40.6	44.9	49.4	61.3	68.7	50.2	55.5	47	50	41.5	45.6
V	185.9	182	232.4	226.2	207	202.6	207.5	202.3	203.1	199	223.8	219.2	197.3	193.2
Co	26.3	26.3	27	28.2	25.6	25.5	24.2	24.2	26.4	26.4	27	28.1	25.9	25.9
Ni	70.9	81.7	65.2	86.9	59.9	69.1	103.8	122.8	82.6	96.1	123	156.6	81.9	94.3
Cu	19.2	17.8	186.7	172	49.5	46	45.1	41.4	56.3	52.1	47	44.1	82.8	77
Zn	65.1	60.4	63.1	58.2	101.5	94.3	80.3	73.6	66.6	61.7	70	65.8	72.7	67.6
Rb	104.4	97	32.1	29.6	88.7	82.4	81.6	74.8	72	66.6	8.6	8.1	72.7	67.6
Sr	555.3	520.8	491.8	457.4	715.7	671.2	673	623.9	842.2	787.1	249.4	235.9	1261.7	1184
Y	16.6	16	16.8	16	17	16.4	17.1	16.4	16.1	15.5	17.3	16.7	17	16.4
Zr	127.2	119.2	127.2	118.2	125.3	117.5	128.3	118.9	120.1	112.2	134.3	127	129.5	121.5
Nb	8.4	7.9	8	7.4	7.6	7.1	8.4	7.8	8	7.5	8.3	7.8	8.5	8
Ba	604	561.1	203.6	187.6	567.2	526.9	612.9	561.9	473.7	438.3	51.8	48.7	6.9	6.4
La	20.7	19.3	22.1	20.4	22.5	20.9	22.5	20.8	19.8	18.4	22.5	21.2	21.8	20.3
Ce	46.2	43.2	48.7	45.1	48.9	45.7	49.7	45.9	44.5	41.5	49.8	47	48.1	45
Nd	26.2	24.7	26.4	24.6	26.8	25.2	26.9	25.1	25.5	24	27.2	25.8	26.7	25.2

Sm	5.3	5	5.2	4.9	5.8	5.5	5.5	5.1	5.3	5	5.8	5.5	5.7	5.4
Eu	1.7	1.6	1.6	1.5	1.7	1.6	1.6	1.5	1.6	1.5	1.7	1.6	1.6	1.6
Gd	5.5	5.2	6.2	5.8	5.4	5.1	5.6	5.3	5	4.8	5.7	5.4	5.4	5.1
Tb	0.7	0.7	0.7	0.6	0.8	0.7	0.7	0.7	0.6	0.6	0.7	0.7	0.7	0.7
Dy	3.4	3.3	3.6	3.4	3.6	3.4	3.6	3.4	3.4	3.2	3.7	3.5	3.6	3.4
Ho	0.6	0.6	0.6	0.6	0.6	0.6	0.6	0.6	0.6	0.6	0.7	0.6	0.7	0.7
Er	1.8	1.7	1.9	1.8	2	1.9	2	1.9	1.8	1.7	2	1.9	2	1.9
Tm	0.2	0.2	0.2	0.2	0.2	0.2	0.2	0.2	0.2	0.2	0.2	0.2	0.2	0.2
Yb	1.4	1.4	1.6	1.5	1.6	1.6	1.6	1.6	1.6	1.5	1.6	1.6	1.7	1.7
Lu	0.2	0.2	0.2	0.2	0.2	0.2	0.2	0.2	0.2	0.2	0.2	0.2	0.2	0.2
Hf	3.5	3.3	3.7	3.4	3.5	3.3	3.5	3.3	3.4	3.2	3.5	3.3	3.5	3.3
Pb	22.8	21.3	9.9	9.1	9.4	8.7	9.3	8.6	8.9	8.3	6.7	6.3	7.7	7.2
Th	3.3	3.1	3.6	3.3	3.5	3.3	3.5	3.2	3.3	3	3.8	3.6	3.6	3.4
U	1.2	1.1	1.3	1.2	1.2	1.1	1.2	1.1	1.2	1.1	1.3	1.2	1.3	1.2
CIPW Norm														
Q	0.69		1.45		4.86	3.36	4.76	3.15			10.40	8.40	7.60	6.01
Or	20.51	19.03	12.94	11.88	16.37	15.19	17.02	15.60	15.90	14.71	2.42	2.30	16.84	15.66
Ab	17.60	16.50	22.42	20.82	19.29	18.11	18.28	17.01	17.35	16.16	14.98	14.13	19.80	18.53
An	14.09	13.58	15.44	14.62	12.80	12.27	13.09	12.43	15.24	14.52	22.63	21.53	10.57	10.20
Di	10.54	11.15	28.24	31.76	17.66	19.98	19.76	22.95	24.08	27.44	26.41	29.36	19.33	21.94
Hy	30.00	33.42	13.10	15.96	22.45	26.26	20.40	23.98	19.88	18.43	15.99	18.60	19.52	22.95
Ol		1.58		0.15					0.63	3.60				
Mt	3.73	2.02	3.76	2.32	3.81	2.22	3.87	2.23	4.02	2.39	4.41	3.03	3.68	2.19
Il	1.42	1.37	1.37	1.29	1.35	1.29	1.33	1.27	1.37	1.29	1.35	1.29	1.25	1.20
Ap	1.21	1.11	1.07	1.00	1.14	1.07	1.23	1.11	1.27	1.18	1.25	1.16	1.14	1.07
Extensive and intensive parameters														
D(g/cm^3)	2.625	2.632	2.615	2.624	2.607	2.614	2.608	2.616	2.641	2.646	2.643	2.65	2.587	2.595
V(poise)	1407	924	925	522	3008	925	1383	797	587	828	609	397	2008	1214
Lg(f_{O2})	-6.2	-7.3	-5.7	-6.7	-6.3	-6.9	-5.8	-6.9	-5.8	-6.8	-4.8	-5.8	-5.8	-6.9
Fractionation phase proportion (wt%)														
Cpx	17.00	22.95	11.02	17.04	16.99	22.94	16.98	23.92	20.94	26.88	18.05	22.12	15.99	21.95
Cr-spinel	0.01	0.06	0.04		0.02	0.07	0.03	0.08	0.07	0.12	0.09	0.14	0.01	0.06
Olivine			0.94	1.87							0.86	1.74		
Melt	83.00	77.00	88.00	80.99	83.00	77.00	83.00	76.00	79.00	73.00	80.99	76.00	84.00	78.00

Initial composition of fractionation phases														
Mg# (cpx)	88.88	90.28	88.17	89.70	88.71	90.02	88.50	90.01	88.65	89.82	88.03	89.18	88.52	89.86
Cr#(spine)	68.67	62.28	54.60	64.90	56.94	67.93	57.72	68.95	57.82	66.08	59.63	66.22	77.42	70.58
Fo(Olivine)			86.15	88.47							86.45	88.14		

Table (II):*Continued:*

Samples	NC-14		NC-015		NC-17		NC-19		NC-53*		NC-54*		NC-56*	
Run	Fe^{3+}/∑Fe 0.32	Fe^{3+}/∑Fe 018	Fe^{3+}/∑Fe 0.32	Fe^{3+}/∑Fe 018	Fe^{3+}/∑Fe 0.32	Fe^{3+}/∑Fe 018	Fe^{3+}/∑Fe 0.32	Fe^{3+}/∑Fe 018	Fe^{3+}/∑Fe 0.32	Fe^{3+}/∑Fe 018	Fe^{3+}/∑Fe 0.32	Fe^{3+}/∑Fe 018	Fe^{3+}/∑Fe 0.32	Fe^{3+}/∑Fe 018
Major oxides (w%)														
SiO_2	54.03	54.1	53.03	52.92	55.07	55.04	54.59	54.39	54.61	54.64	55.05	55.02	55.01	54.76
TiO_2	0.71	0.67	0.74	0.7	0.72	0.68	0.67	0.63	0.74	0.71	0.73	0.69	0.73	0.7
Al_2O_3	12.31	11.5	12.99	12.05	11.6	10.83	11.44	10.67	12.57	11.89	12.27	11.48	12.26	11.7
Fe_2O_3	2.71	1.56	3.5	2.2	2.75	1.61	2.81	1.73	2.56	1.48	2.64	1.49	2.65	1.53
FeO	6.39	7.1	5.83	6.71	6.28	6.99	5.8	6.52	6.05	6.81	6.28	7.08	6.3	7.02
MnO	0.13	0.11	0.13	0.12	0.12	0.11	0.12	0.11	0.12	0.11	0.13	0.14	0.15	0.14
MgO	9.2	10.32	8.5	9.64	9.11	10.19	8.4	9.48	8.8	9.82	9.03	10.26	9.03	10.03
CaO	8.76	9.29	12.07	12.68	8.77	9.37	11.02	11.66	8.51	8.91	7.96	8.36	7.95	8.3
Na_2O	2.16	2	2.3	2.11	2.02	1.87	2.48	2.3	2.13	2	2.15	1.99	2.15	2.46
K_2O	2.79	2.56	0.2	0.19	2.71	2.48	1.9	1.75	3.14	2.93	3.04	2.79	3.03	2.68
P_2O_5	0.53	0.49	0.53	0.48	0.52	0.47	0.51	0.47	0.44	0.41	0.43	0.39	0.43	0.41
Cr_2O_3	0.04	0.06	0.04	0.08	0.04	0.06	0.05	0.08	0.03	0.05	0.03	0.05	0.03	0.04
Total	99.76	99.76	99.86	99.88	99.71	99.7	99.79	99.79	99.7	99.76	99.74	99.74	99.72	99.77
Trace element abundances (ppm)														
Sc	42.1	47.1	31.7	34.6	44.5	49.8	45.2	49.1	26.9	29.6	26.9	30	26.8	31.7
V	219.7	214.2	237.7	231.2	191.7	187.2	203.9	198.2	209.6	205	211.6	206.1	211.5	214.3
Co	24.6	24.6	89.8	95.2	28.3	28.3	26.7	28.2	30.3	30.3	33.7	33.6	33.7	27.3
Ni	83.8	99.1	98.6	138.9	89.2	105.5	84.8	116.1						
Cu	57.6	52.8	67.9	62.1	42.4	38.9	32.5	29.9	20.3	18.9	27.8	25.5	27.8	24.6
Zn	64.3	58.9	66.1	60.4	64.9	59.5	64.1	59	33	30.7	33.7	31	33.7	28.6
Rb	68.2	62.5	3.8	3.5	82.4	75.6	52.1	48	88.8	82.7	87.8	80.6	87.7	67.6
Sr	659.9	611.8	31.7	29.3	1038.9	963.1	593.1	551.2	1017.5	955.6	1065	988.5	1064.2	500.1
Y	15.8	15.1	16	15.2	17.2	16.5	16.5	15.8	18.5	17.8	18.6	18	18.8	18.3
Zr	123.8	114.7	129.9	119.9	124.2	115.1	123.3	114.6	154.3	144.9	151.4	140.5	151.3	137.9
Nb	7.6	7	7.5	6.8	7.6	7	7.4	6.8	8.5	8	8.5	7.8	8.5	8
Ba	460.7	422.4	31.5	28.8	536.3	491.7	400.9	369.2	588.3	547.5	505.1	463.8	504.7	579.8
La	20.7	19.1	22.4	20.5	21.5	19.8	20.5	19	26.3	24.6	26	24	26	24.4
Ce	44.6	41.2	48.8	44.9	47.5	43.9	45.5	42.2	50.9	47.7	50.9	47.1	50.8	47.7
Nd	25.4	23.7	27.3	25.3	26.3	24.5	25.1	23.4	30	28.3	30.2	28.1	30.1	29.1

Sm	5.1	4.8	5.5	5.1	5.7	5.4	5.4	5.1	6.4	6.1	6.5	6.1	6.4	6.2
Eu	1.6	1.5	1.5	1.4	1.6	1.5	1.6	1.5	1.8	1.7	1.8	1.7	1.8	1.7
Gd	5.3	5	5.4	5.1	5.2	4.9	5.2	5	5.5	5.2	5.7	5.4	5.7	5.5
Tb	0.7	0.6	0.7	0.6	0.8	0.7	0.7	0.6	0.7	0.7	0.7	0.7	0.7	0.7
Dy	3.3	3.2	3.6	3.4	3.5	3.4	3.3	3.2	4	3.9	4.2	4	4.2	4.1
Ho	0.6	0.6	0.6	0.6	0.6	0.6	0.6	0.6	0.7	0.7	0.7	0.7	0.7	0.7
Er	1.8	1.7	1.8	1.7	1.9	1.8	1.8	1.7	1.9	1.8	1.9	1.8	1.9	2
Tm	0.2	0.2	0.2	0.2	0.2	0.2	0.2	0.2	0.3	0.3	0.3	0.3	0.3	0.3
Yb	1.4	1.4	1.6	1.5	1.4	1.4	1.6	1.5	1.8	1.7	1.9	1.8	1.9	1.7
Lu	0.2	0.2	0.2	0.2	0.2	0.2	0.2	0.2	0.3	0.3	0.3	0.2	0.3	0.3
Hf	3.5	3.3	3.8	3.5	3.5	3.3	3.4	3.2	3.5	3.3	3.5	3.3	3.5	3.4
Pb	8.5	7.8	8.4	7.7	7.6	7	15.7	14.5	4.3	4	5.1	4.7	5.1	4.8
Th	3.2	2.9	3.4	3.2	3.5	3.2	3.3	3.1	4.3	4	4.3	4	4.3	4.1
U	1.1	1	1.2	1.1	1.2	1.1	1.2	1.1	1.1	1	1.10	1.00	1.10	1
CIPW Norm														
Q	1.15		5.62	3.35	3.78	2.30	2.77	0.99	1.61	0.29	2.50	1.05	2.48	
Or	16.49	15.13	1.18	1.12	16.02	14.66	11.23	10.34	18.56	17.32	17.97	16.49	17.91	15.84
Ab	18.28	16.92	19.46	17.85	17.09	15.82	20.98	19.46	18.02	16.92	18.19	16.84	18.19	20.82
An	15.65	14.84	24.53	22.85	14.58	13.83	14.47	13.62	15.46	14.81	14.85	14.15	14.85	12.97
Di	19.59	22.64	25.57	29.76	20.54	23.87	29.63	33.19	19.21	21.56	17.57	20.00	17.53	20.62
Hy	22.08	25.21	15.78	19.28	21.14	24.48	14.17	17.36	20.71	24.40	22.45	26.82	22.54	23.05
Ol		0.32												1.98
Mt	3.93	2.26	5.07	3.19	3.99	2.33	4.07	2.51	3.71	2.15	3.83	2.16	3.84	2.22
Il	1.35	1.27	1.41	1.33	1.37	1.29	1.27	1.20	1.41	1.35	1.39	1.31	1.39	1.33
Ap	1.23	1.14	1.23	1.11	1.21	1.09	1.18	1.09	1.02	0.95	1.00	0.90	1.00	0.95
Extensive and intensive parameters														
D(g/cm^3)	2.629	2.635	2.659	2.666	2.621	2.628	2.62	2.63	2.615	2.622	2.615	2.62	2.616	2.621
V(poise)	974	589	525	596	1022	608	644	370	1335	853	1390	824	1382	840
Log(f_{O2})	-5.9	-6.9	-4.7	-5.8	-5.7	-6.8	-5.5	-6.6	-5.9	-7	-5.9	-7	-5.9	-7.1
Fractionation phase proportion (wt%)														
Cpx	16.97	23.91	3.57	10.58	16.97	23.90	19.49	24.67	14.98	20.94	14.99	21.94	14.99	
Cr-spinel	0.04	0.09	0.05	0.14	0.04	0.10	0.08	0.13	0.03	0.06	0.02	0.06	0.02	0.06

Olivine			4.38	5.29			traces	1.20						
Melt	83.00	83.00	92.00	84.00	83.00	76.00	80.44	73.99	84.99	79.00	84.99	78.00	84.99	80.00
Initial composition of fractionation phases														
Mg# (cpx)	88.56	90.01	87.55	89.18	88.54	89.97	88.24	89.71	88.67	89.96	88.58	90.05	88.53	89.88
Cr#(spine)	53.57	65.07	48.35	0.34	57.83	68.22	60.73	69.39	50.97	61.39	68.58	64.85	68.53	62.49
Fo(Olivine)			86.87	88.25			86.62	88.78						

*data published in Nicholson et al. (2011)

c. Tests of reverse crystallization modelling

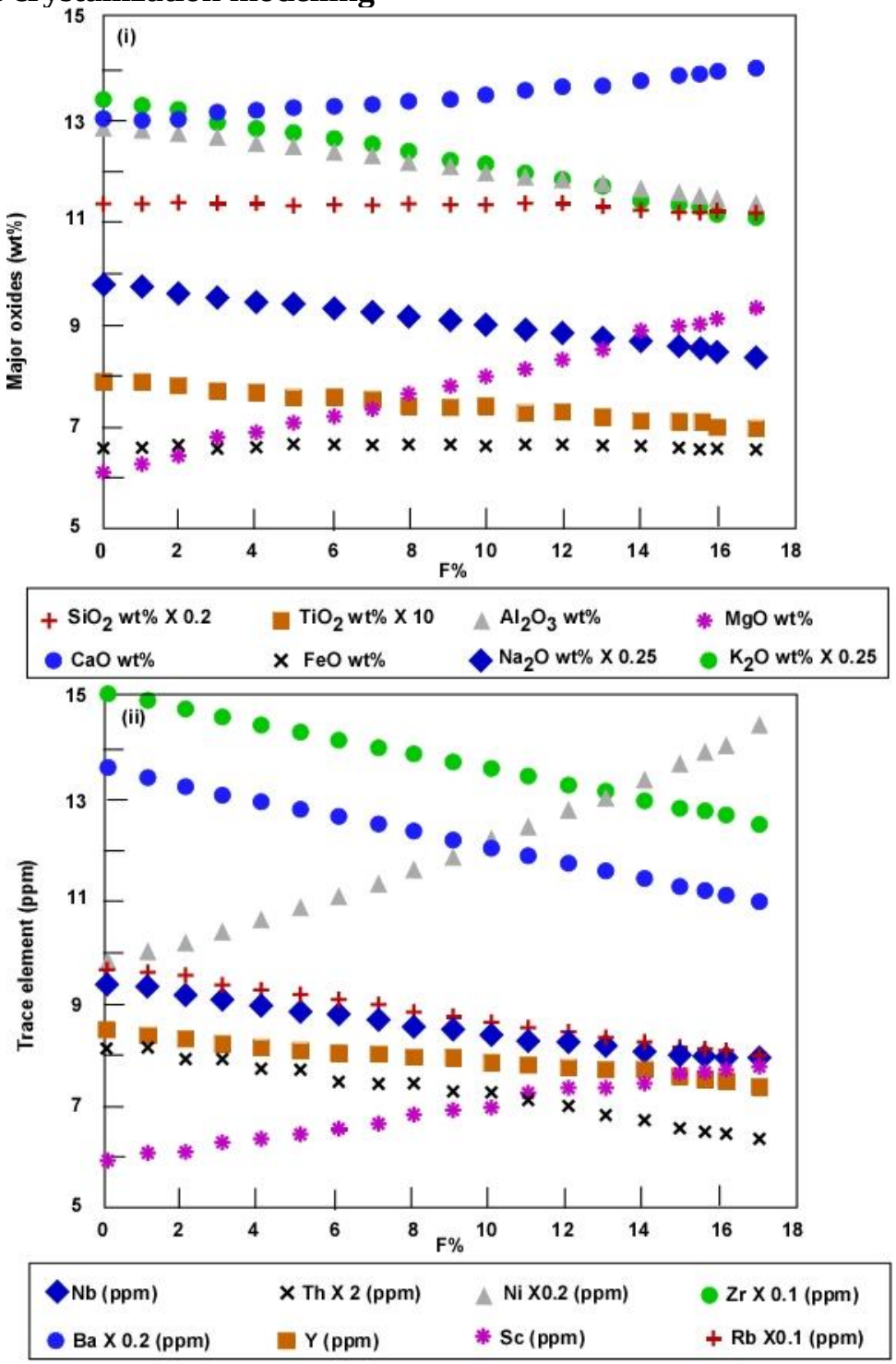

Fig. (B 2a) Major and trace elements abundance of the melt fractions resulting from reverse fractionation modeling for Sample NC-01as an example of La Conception lavas. The abundances of elements in the melt fractions calculated under both oxidizing and reducing conditions are broadly similar,

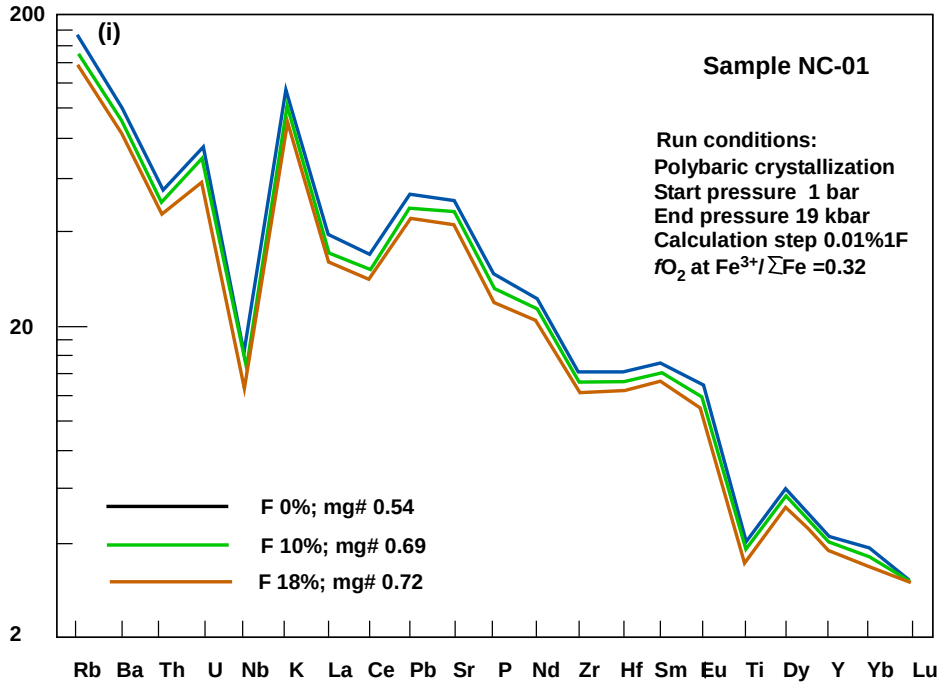

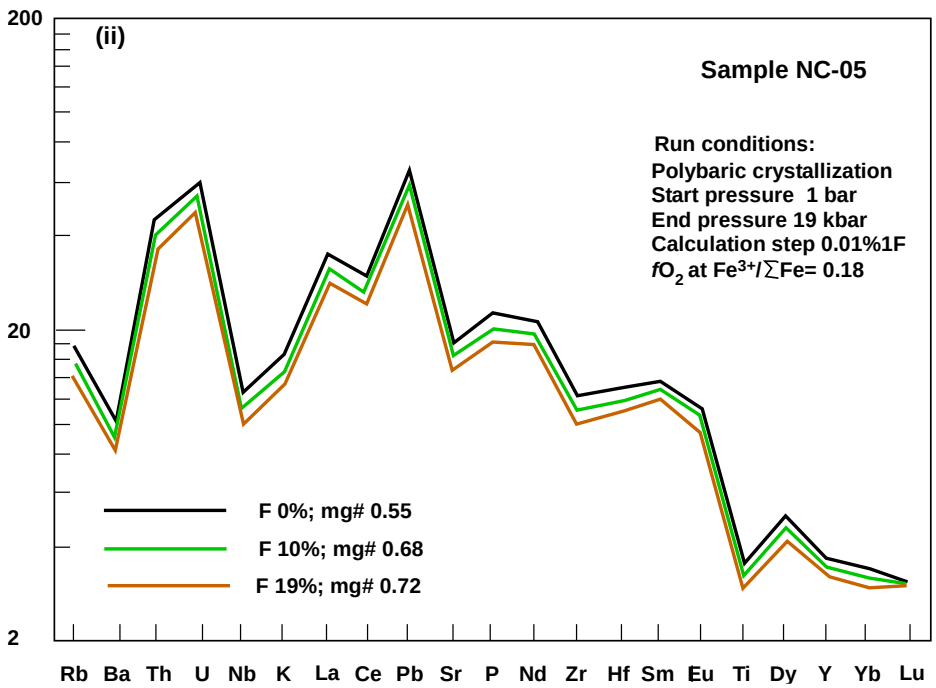

Fig. (B 2b) Primitive-mantle normalized patterns of melt fractions resulting from reverse fractionation modeling of samples NC-01 and NC-05 under oxidizing (fO_2 buffered $Fe^{3+}/\sum Fe$ =0.32); and (fO_2 buffered $Fe^{3+}/\sum Fe$ =0.18), respectively. Normalized values are those of McDonough and Sun (1995). For more details, see the main text.

(b,

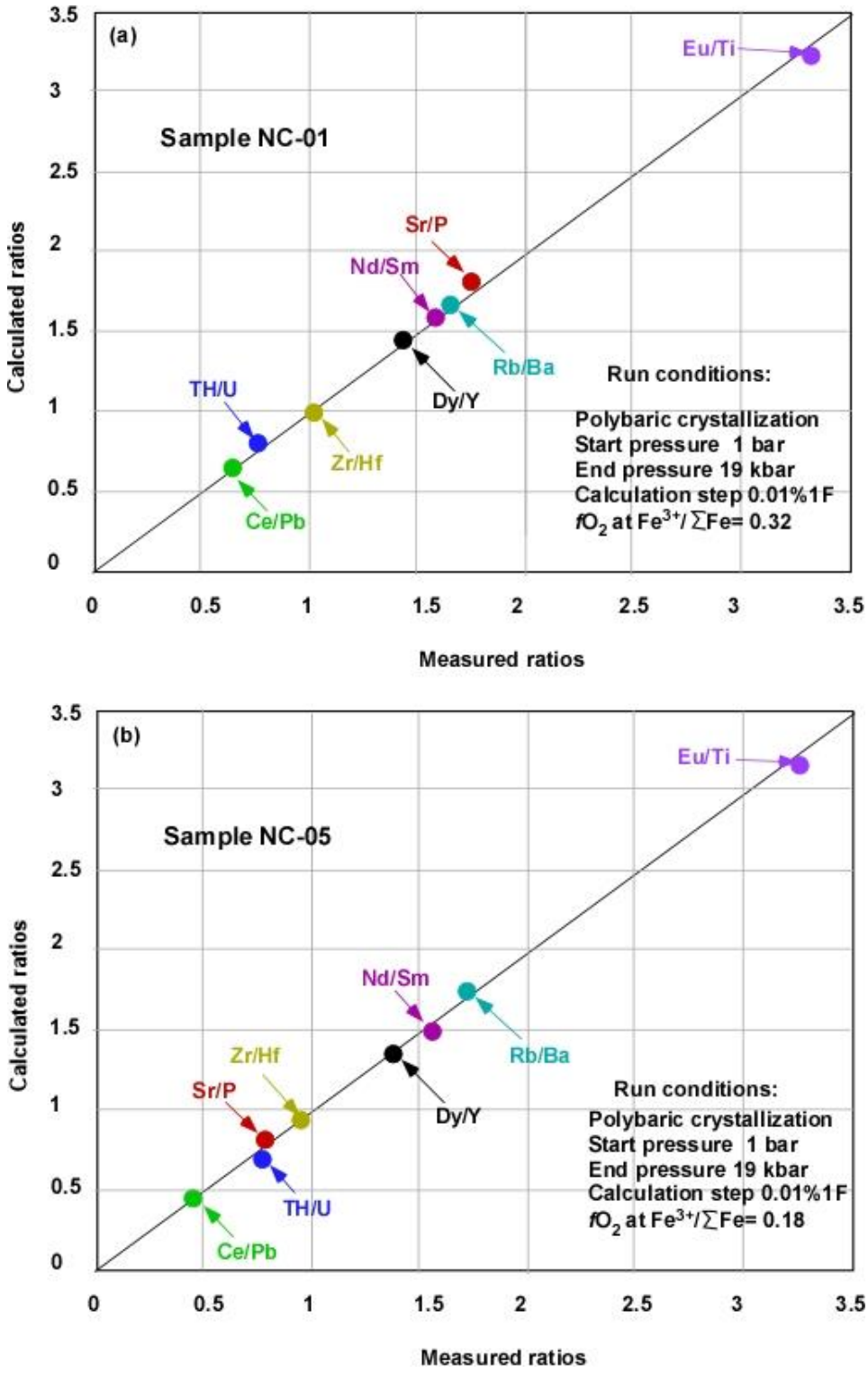

Fig. (B 2c) Plots showing the conservative behavior of the incompatible trace element ratios during fractional crystallization of Samples NC-01 and NC-05. All values are normalized primitive mantle after McDonough and Sun (1995). For more details, see the main text.

Appendix C
Estimation of the Subduction components

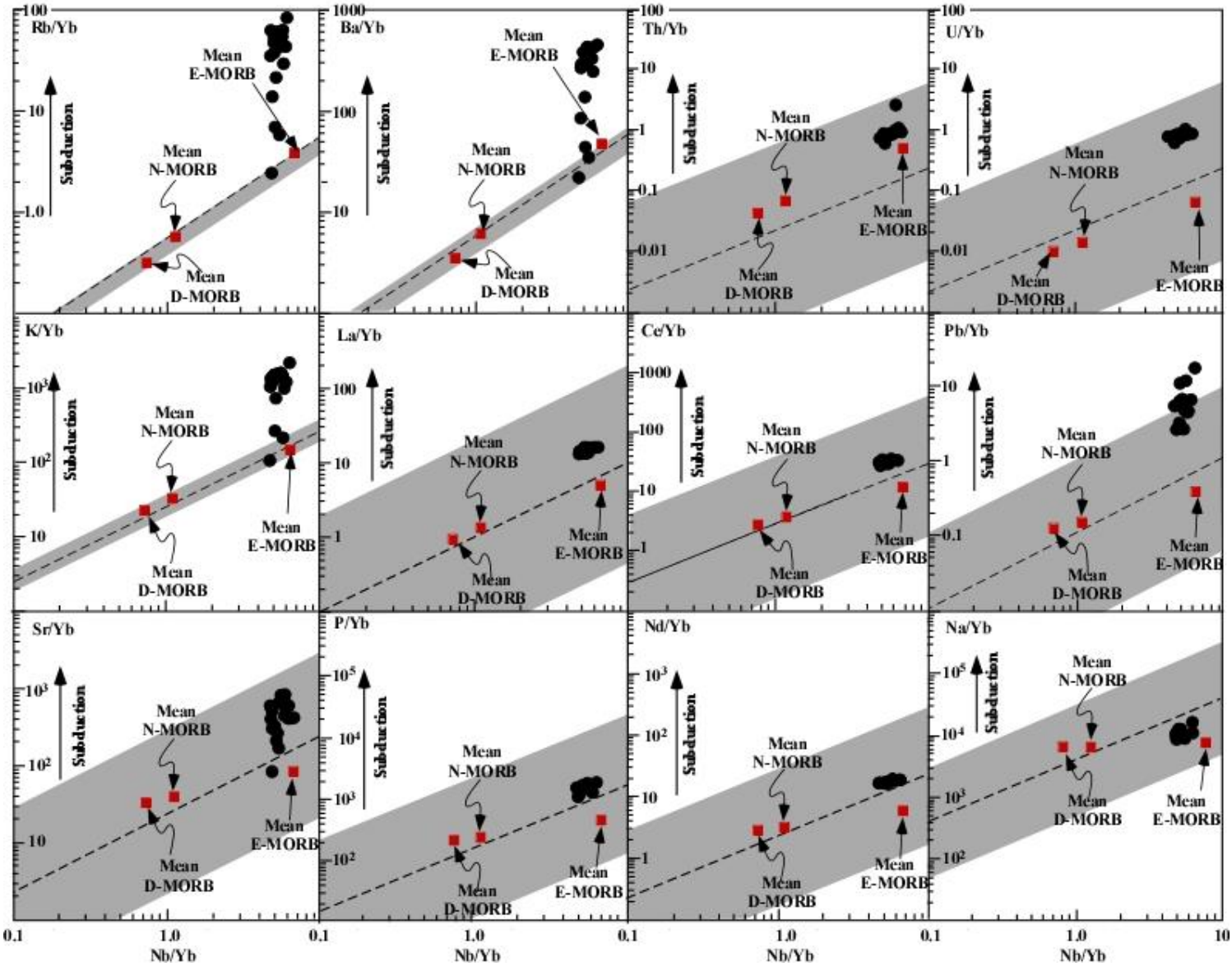

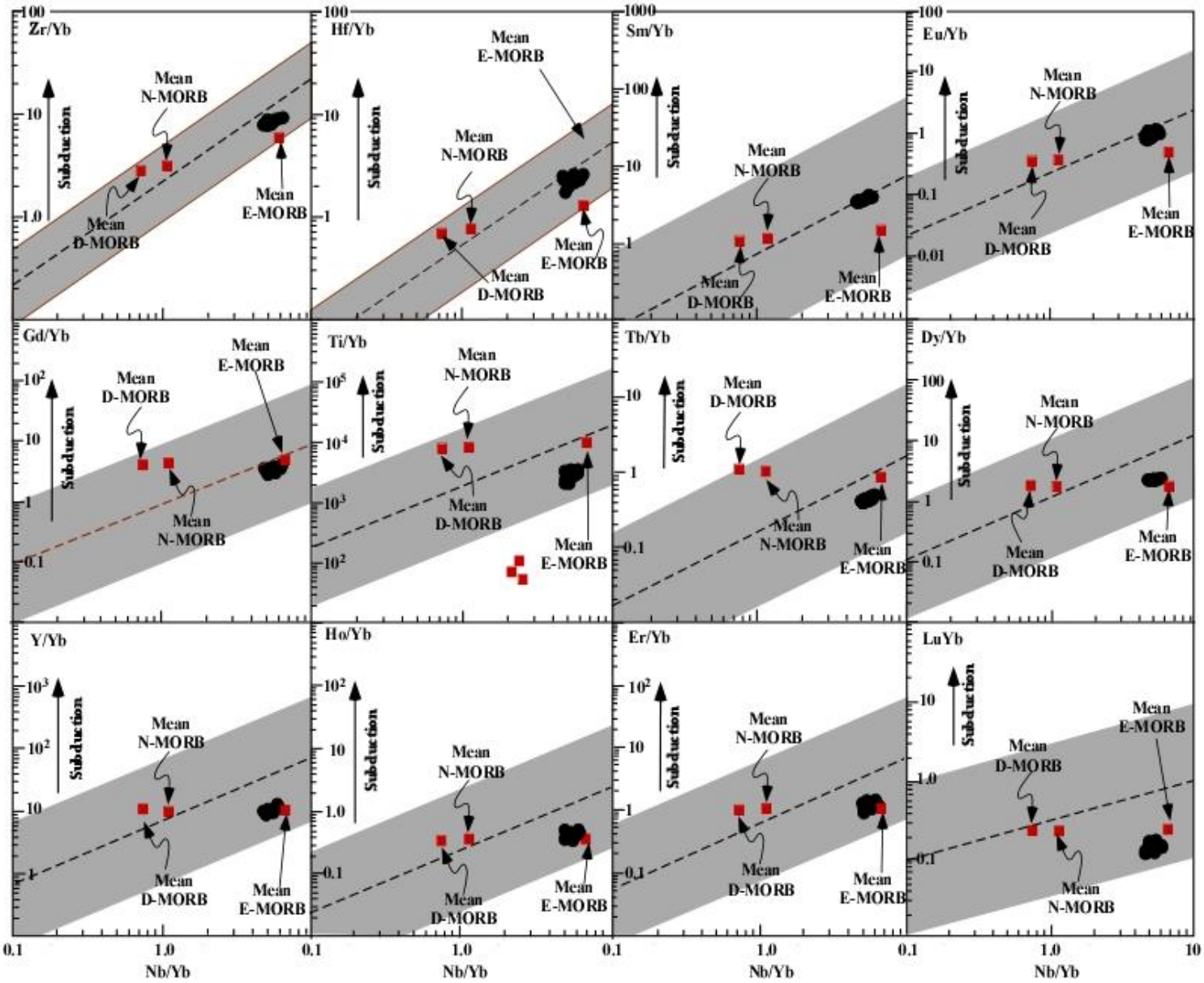
Zr/Yb
Hf/Yb
Sm/Yb
Eu/Yb
Gd/Yb
Ti/Yb
Tb/Yb
Dy/Yb
Y/Yb
Ho/Yb
Er/Yb
LuYb
Subduction
Mean N-MORB
Mean D-MORB
Mean E-MORB
Nb/Yb

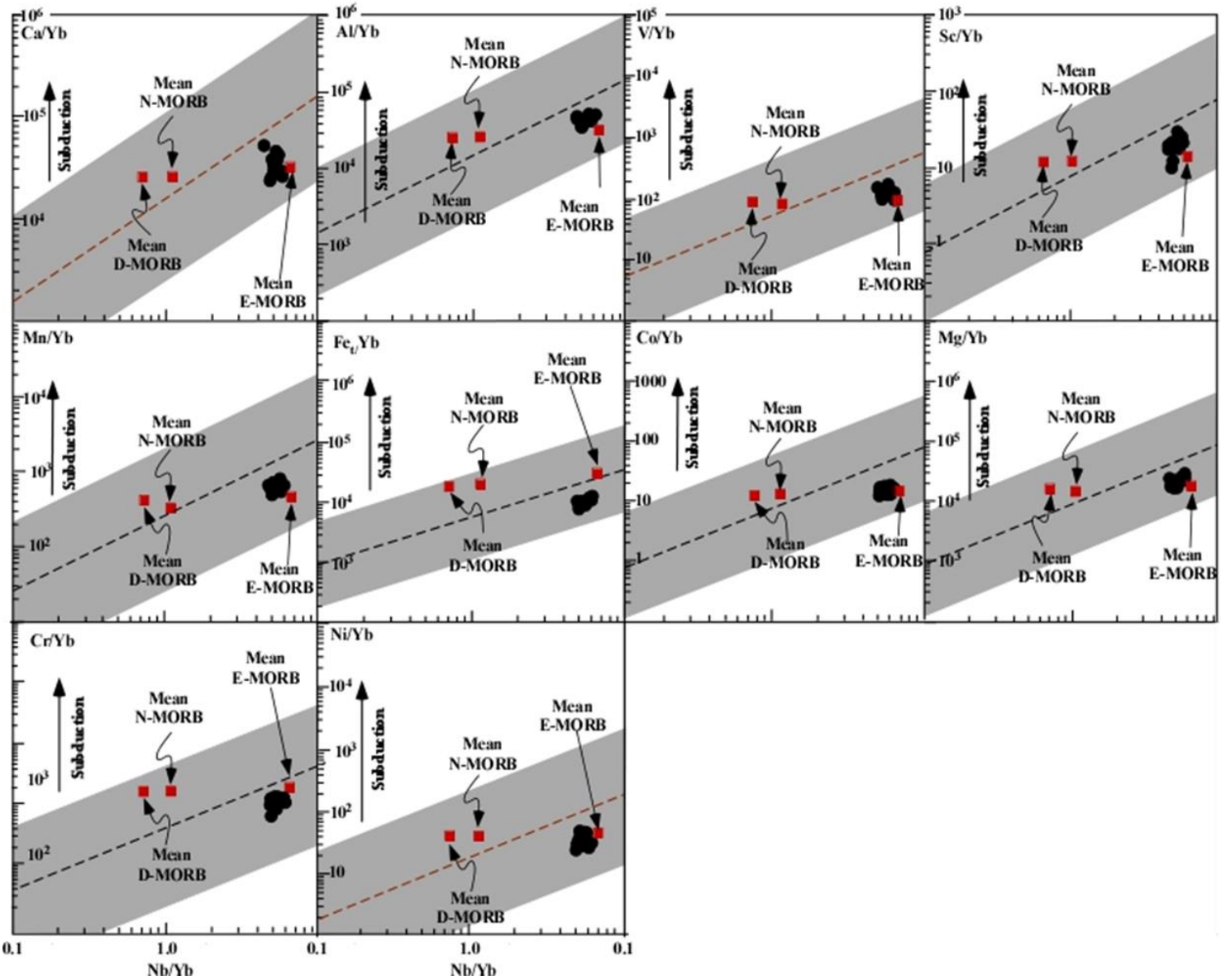

Figure C1. Bivariate proxy plots illustrating the conservative and non-conservator elements in the La Conception Lava. N-MORB, D-MORB (La/Sm_N<0.8) and E-MORB (La/Sm_N>1.5) are respectively the log-normal mean, weighted by segment length of the normal MORB, depleted MORB and enriched MORB, respectively. Shaded fields represent MORB array. The upper and lower bounds bracket the composition of 95% of the sampled ridge length. The dashed lines are the mean of MORB at given Nb/Yb. All data are from (Gale et al., 2013).

Table (III) The percentage of the subduction component (%sz) of the elements in the La Conception estimated from the displacement from the average MORB at given Nb.

Sample	Rb	Ba	Th	U	K	La	Ce	Pb	Sr	P	Nd	Na	Zr	Hf	Sm	Eu	Gd
NC-01	94	92	95	85	91	60	49	86	76	41	25	-95	-49	-33	-18	-33	-60
NC-02	95	93	86	86	92	64	54	90	75	46	33	-38	-38	-20	1	-28	-51
NC-03	95	92	87	87	92	67	57	90	78	47	33	-36	-30	-20	-4	-20	-37
NC-04	92	90	87	87	89	64	53	90	65	32	28	-27	-45	-33	-14	-40	-60
NC-05	56	32	85	85	47	65	54	91	44	39	31	-40	-42	-20	-4	-23	-46
NC-06	95	92	85	85	91	63	51	89	76	41	26	-53	-47	-33	-14	-43	-55
NC-07	96	92	84	84	93	60	48	96	62	43	24	-98	-50	-33	-22	-37	-56
NC-08	86	78	86	86	82	64	53	91	59	40	29	-47	-42	-20	-15	-33	-52
NC-09	95	93	86	86	92	66	56	91	73	46	33	-64	-38	-20	1	-26	-44
NC-10	94	92	85	85	91	63	52	90	69	44	26	-91	-49	-33	-18	-44	-51
NC-11	94	91	84	84	91	60	48	90	76	49	25	-91	-52	-33	-18	-41	-64
NC-12	46	11	86	86	38	63	52	86	17	46	28	-128	-40	-33	-10	-35	-49
NC-13	93	93	85	85	91	61	49	88	83	39	25	-79	-49	-33	-14	-41	-60
NC-14	94	91	85	85	92	64	51	90	71	50	30	-71	-38	-20	-13	-30	-46
NC-15	-10	-32	86	86	-11	67	57	90	-37	50	37	-56	-28	-6	-1	-27	-32
NC-16	80	67	86	86		64	54	90	69		30		-38	-42	-8	-39	-43
NC-17	95	92	86	86	92	65	55	89	82	49	32	-82	-38	-20	-1	-26	-47
NC-18	92	90	86	86		63	53	95	31		31		-37	-20	-3	-34	-49
NC-19	92	90	86	86	88	64	54	95	69	50	30	-45	-36	-20	-4	-27	-44
NC-00	89	87	85	85	86	61	50	90	73	42	23	-95	-45	-33	-16	-40	-57
NC56*	93	92	82	82	91	67	51	83	59	31	34	-62	-34	-25	-1	-31	-50
NC54*	94	90	82	82	91	66	50	80	79	28	31	-100	-32	-32	-4	-33	-54
NC53*	94	92	82	82	92	67	51	80	78	30	31	-102	-29	-32	-4	-34	-62

Table (III) ***Continued:***

Sample	Ti	Tb	Dy	Y	Ho	Er	Lu	Ca	Al	V	Sc	Mn	Fe	Co	mg	Cr	Ni
NC-01	-181	-87	-163	-179	-196	-204	-224	-234	-50	-206	-123	-134	-162	-217	-136	-107	-204
NC-02	-155	-71	-155	-153	-163	-194	-161	-195	-32	-147	-101	-110	-141	-183	-110	-86	-172
NC-03	-139	-73	-143	-138	-127	-179	-192	-177	-27	-150	-101	-105	-136	-191	-120	-86	-193
NC-04	-182	-85	-166	-170	-184	-217	-190	-212	-114	-189	-123	-153	-187	-205	-132	-107	-204
NC-05	-162	-75	-154	-158	-163	-213	-232	-90	-101	-134	-107	-119	-146	-192	-118	-104	-168
NC-06	-167	-87	-168	-166	-176	-243	-212	-200	-102	-171	-117	-129	-166	-207	-132	-116	-162
NC-07	-161	-95	-180	-176	-196	-250	-238	-246	-100	-196	-123	-137	-153	-211	-122	-116	-201
NC-08	-154	-92	-147	-154	-179	-203	-181	-102	-86	-119	-114	-116	-147	-187	-112	-114	-203
NC-09	-147	-65	-143	-144	-174	-188	-204	-187	-94	-141	-95	-120	-149	-190	-115	-94	-203
NC-10	-180	-83	-168	-169	-200	-217	-224	-198	-114	-167	-58	-151	-179	-209	-144	-90	-141
NC-11	-163	-111	-177	-178	-200	-233	-238	-158	-98	-168	-105	-130	-153	-210	-128	-98	-201
NC-12	-172	-83	-161	-164	-180	-208	-212	-117	-108	-149	-111	-134	-169	-219	-141	-126	-141
NC-13	-198	-102	-172	-172	-169	-224	-212	-228	-130	-181	-130	-125	-193	-216	-154	-138	-198
NC-14	-148	-82	-161	-161	-166	-218	-192	-148	-79	-127	-107	-113	-139	-199	-103	-104	-168
NC-15	-125	-69	-123	-138	-155	-198	-195	-43	-62	-91	-96	-96	-126	-181	-91	-81	-199
NC-16		-69	-146	-161	-164	-216	-241			-146	-96			-197		-73	-154
NC-17	-145	-63	-143	-139	-159	-192	-204	-151	-90	-159	-95	-106	-140	-160	-103	-78	-151
NC-18		-85	-148	-155	-163	-213	-192			-133	-101			-187		-78	-126
NC-19	-157	-77	-156	-147	-152	-210	-204	-120	-88	-143	-101	-114	-147	-177	-118	-86	-182
NC-00	-166	-97	-168	-179	-165	-229	-238	-129	-101	-161	-117	-132	-141	-209	-123	-107	-204
NC56*	-173	-88	-129	-147	-146	-221	-176	-201	-104	-156	-224	-96	-175	-200	-117	-149	
NC54*	-179	-99	-135	-156	-157	-248	-189	-202	-109	-170	-240	-140	-180	-176	-132	-144	
NC53*	-175	-96	-148	-157	-168	-246	-187	-184	-103	-172	-250	-137	-190	-177	-137	-149	

Appendix D

The concentration of an element in melts derived from mantle peridotites was estimated from melting equations 13 and 15 of Shaw (1970):

$$\frac{C_l^i}{C_0^i} = \frac{1}{D_i^0}\left(1 - \frac{PF}{D_i^0}\right)^{\left(\frac{1}{P}-1\right)}$$ *for non-modal polybaric fractional melting*

$$\frac{C_l}{C_0} = \frac{L}{D_i^0 + F(1-P)}$$ *for non-modal isobaric batch melting*

where,

C_l^i *= concentration of i in the melt fraction.*

C_0^i *= concentration of i in the primitive mantle source Table IV) after of McDonough & Sun, (1995).*

D_i^o *= bulk distribution coefficient of i in the original source calculated using mineral/melt partition in Table(V) and the mineral proportions in the initial source and (VI)*

P = bulk distribution coefficient of the phases which enter melt and calculated from mineral/melt partition coefficient listed in Table V and the melting coefficients listed in Walter (1999) and Walter (1998) for spinel and garnet-stability field respectively.

In batch melting, solid and liquid fractions remain together throughout the entire melting interval, while in fractional melting infinitesimal increments of melting occur, accompanied by instantaneous segregation of the melt from the solid residue. The concentration of an element in the solid residue of the polybaric, near fractional melting, represents the end-product of a complex series of melting reactions that change as a function of pressure, temperature and bulk composition (e.g., Johnson

et al., 1990 Takazawa et al., 2000). The abundance of a trace element was therefore calculated at 1 kbar pressure increment for each sequentially depleted bulk composition. This melt production rate is in the range estimated for melting at oceanic ridge (e.g., Iwamori et al., 1995), although the melting rate is probably not constant during melting interval (Asimov et al., 1997; Yang et al., 1998). For polybaric near fractional melting within spinel stability field (25 to 11 kbar), the calculations were performed using melting coefficients by Walter (1999) whereas the polybaric near fractional melting within garnet stability field (40 to25 kbar) were carried out using melting coefficients by Walter (1998).

Table (IV) Trace element abundances (ppm) of the primitive mantle (after McDonough & Sun,1995)

Element	Zr	Nb	Nd	Y	Gd	Dy	Yb
(ppm)	10.5	0.713	1.25	4.3	0.644	0.674	0.441

Table (V) Mineral/mineral partition coefficients used in the modeling of melting mantle peridotite

Element	Zr	Nb	Nd	Y	Dy	Yb
Olivine	0.0005	0.0001	0.00007	0.0036	0.004	0.023
Opx	0.014	0.003	0.009	0.19	0.060	0.100
Cpx	0.1234	0.0077	0.1873	0.467	0.442	0.43
Spinel	0.07	.01	0.0006	0.0001	0.0015	0.0045
Garnet	0.27	0.0031	0.052	3.1	2.2	6.6

Cpx/melt partition coefficients are from Hart and Dunn (1993); garnet/melt partition coefficients are from Johnson (1998). Partition confidences of olivine/melt, opx/melt and spinel/melt are from Kelemen et al. (1993); except values for Y their partition coefficients are respectively from Nielsen et al, (1992) for olivine; from Dunn and Sen (1994) for opx and from Wijbrans et al. (2015) for spinel.

Table (VI) Mineral proportions in the initial source

Mineral proportions	Olivine	Opx	Cpx	Spinel	Garnet
Spinel peridotite[a]	0.538	0.143	0.292	0.027	----------
Garnet peridotite[b]	0.537	0.155	0.267		0.041

[a]Mineral proportion of the fertile spinel peridotite (i.e. model lherzolite A mode) after Walter (1999).

[b] Mineral proportion of the fertile garnet peridotite at 35 kbar interpolated from Walter 'data (1998).

Appendix E

Table (VIIA): Intensive and extensive melting parameters calculating from the composition of the La Conception lavas assuming 0 wt% of their pre-eruptive H_2O content

Parameter	Melting temperatures (T_{Ol-L})				Potential temperatures		Pressure	Melting fraction	
Reference	Lee et al (2009)	Beattie (1993)	Putirka et al. (2007)	Putirka (2016)	Putirka. (2016)	Putirka. (2016)	Lee et al. (2009)	Putirka (2016)	Putirka et al. (2007)
	Tm (ºC)	Tm (ºC)	Tm (ºC)	Tm (ºC)	Tp (ºC)[1]	Tp (ºC)[2]	P(GPa)1	Fm %	Fm %*
NC-00	(1242-1264)	(1258-1269)	(1241-1261)	(1258-1268)	(1248-1281)	(1244-1273)	(0.53-0.53)	(1-9)	(<1-3)
NC-01	(1236-1266)	(1292-1315)	(1258-1290)	(1291-1314)	(1291-1338)	(1278-1320)	(0.33-0.38)	(2-9)	(7-12)
NC-02	(1236-1258)	(1304-1320)	(1269-1292)	(1302-1317)	(1289-1325)	(1281-1312)	(0.55-0.58)	(<1-6)	(4-8)
NC-03	(1240-1266)	(1302-1319)	(1270-1296)	(1300-1316)	(1286-1326)	(1279-1315)	(0.61-0.64)	(<1-7)	(3-8)
NC-04	(1216-1246)	(1279-1298)	(1245-1274)	(1278-1296)	(1265-1310)	(1256-1296)	(0.65-0.68)	(2-10)	(4-10)
NC-05	(1234-1260)	(1247-1267)	(1229-1232)	(1246-1266)	(1243-1225)	(1236-1227)	(0.68-0.73)	(1-3)	(<1-<1))
NC-06	(1234-1268)	(1302-1325)	(1267-1301)	(1299-1322)	(1274-1340)	(1270-1325)	(0.65-0.70)	(<1-5)	(<1-7)
NC-07	(1257-1292)	(1337-1366)	(1297-1333)	(1334-1361)	(1324-1381)	(1313-1364)	(0.51-0.58)	(<1-2)	(3-9)
NC-08	(1208-1237)	(1239-1263)	(1217-1249)	(1239-1262)	(1223-1281)	(1220-1268)	(0.56-0.61)	(2-8)	(<1-4)
NC-09	(1227-1255)	(1283-1304)	(1250-1279)	(1282-1302)	(1287-1342)	(1272-1318)	(0.38-0.43)	(3-9)	(6-11)
NC-10	(1221-1252)	(1271-1293)	(1241-1272)	(1271-1292)	(1272-1331)	(1259-1309)	(0.35-0.40)	(2-10)	(4-10)
NC-11	(1252-1275)	(1297-1311)	(1271-1294)	(1295-1309)	(1282-1326)	(1277-1314)	(0.62-0.64)	(<1-5)	(<1-3)
NC-12	(1221-1244)	(1211-1230)	(1198-1224)	(1211-1230)	(1235-1280)	(1219-1257)	(0.35-0.38)	(7-11)	(2-5)
NC-13	(1206-1233)	(1258-1277)	(1225-1253)	(1258-1277)	(1275-1328)	(1255-1299)	(0.23-0.27)	(7-10)	(9-13)
NC-14	(1239-1269)	(1293-1314)	(1263-1293)	(1291-1311)	(1277-1333)	(1271-1318)	(0.55-0.59)	(<1-5)	(<1-6)
NC-15	(1229-1261)	(1230-1257)	(1214-1249)	(1230-1256)	(1217-1277)	(1215-1266)	(0.70-0.75)	(<1-6)	(<1-<1)
NC-17	(1233-1262)	(1279-1299)	(1250-1280)	(1278-1297)	(1275-1332)	(1265-1313)	(0.41-0.46)	(1-8)	(3-8)
NC-19	(1221-1251)	(1247-1270)	(1226-1258)	(1246-1269)	(1244-1301)	(1236-1284)	(0.55-0.60)	(3-10)	(<1-5)
NC-53	(1227-1254)	(1282-1302)	(1250-1279)	(1280-1300)	(1266-1318)	(1259-1303)	(0.45-0.50)	(<1-5)	(2-7)
NC-54	(1230-1263)	(1288-1313)	(1255-1289)	(1286-1311)	(1276-1337)	(1267-1319)	(0.44-0.49)	(<1-6)	(2-8)
NC-56	(1231-1258)	(1288-1318)	(1255-1291)	(1287-1315)	(1276-1329)	(1267-1315)	(0.44-0.64)	(<1-4)	(2-7)

The parameters are calculated assuming anhydrous composition. Melting temperatures (T*m*)are calculated from Ol-liquid thermometers of the Lee *et al.* (2009) equation 3; Beattie (1993) equation 10; Putirka *et al.* (2007) equation 4 and Putirka (2016) equation 13. T*p* ºC[1] and T*p* ºC1 [2] are potential temperature calculated using Tm estimated from Putirka et al. (2007) geothermometry and assuming constant and variable $\Delta H_{fus}/C_p$ and $V\alpha T/C_p$, respectively (equation. 2C, Putirka (2016**).** Pm (GPa)[1] is the e melting pressures calculated from geobaromter of Lee *et al*. (2009) equation 2. First and second Figures between the brackets are for fractionation-corrected melts under oxidizing and reducing conditions, respectively. Fm % is the melt fraction percent estimated from Putirka (2016) eq. 14b; Putirka *et al*., (2007) eq. A* and A2**; Lee and Chin (2014; eq. 7). Fe_2O_3/FeO values are calculated using

Putirka (2016) eq. 6b fO_2 values are calculated using the model of Fegley, (2013); mantle olivine composition and K_D (Fe-Mg) are calculated using the spreadsheet of Putirka (2016) (http://www.minsocam.org/ MSA/AmMin/ TOC/).

Table (VIIA): *Continued*

Parameter	Melting fraction		Melting redox state			Calculated mantle Olivine Composition			
Reference	Putirka et (2007)	Lee & Chin (2014)	Putirka (2016)	Fegley (2013)		Putirka (2016)			
	Fm %**	Fm %	Fe_2O_3/FeO	log fO_2	ΔQFM	SiO_2 wt %	FeO_t wt %	MgO wt%	K_D(Fe-Mg)
NC-00	(4-8)	(8-9)	(0.283-0.175)	(-7.46 – -7.37)	(-0.10 – -0.22)	(40.25-40.51)	(13.10-11.74)	(46.65-47.76)	(0.344-0.345)
NC-01	(11-16)	(15-18)	(0.301-0.181)	(-7.22 – -6.97)	(-0.10 – -0.21)	(40.32-40.58)	(12.71-11.35)	(46.96-48.07)	(0.346-0.347)
NC-02	(9-12)	(13-15)	(0.302-0.198)	(-6.96 – -6.80)	(-0.03 – -0.07)	(40.41-40.61)	(12.22-11.20)	(47.36-48.19)	(0.343-0.344)
NC-03	(7-12)	(12-14)	(0.290-0.181)	(-6.94 – -6.77)	(+0.04 – -0.08)	(40.43-40.66)	(12.13-10.92)	(47.44-48.42)	(0.342-0.344)
NC-04	(8-13)	(10-12)	(0.314-0.196)	(-7.24 – -7.05)	(-0.07 – -0.21)	(40.38-40.67)	(12.42-10.88)	(47.20-48.46)	(0.344-0.345)
NC-05	(<1-6)	(8-10)	(0.294-0.153)	(-7.66 – -7.40)	(+0.11 – -0.33)	(40.18-40.53)	(13.46-11.60)	(46.35-47.87)	(0.347-0.334)
NC-06	(5-11)	(10-14)	(0.315-0.186)	(-6.88 – -6.66)	(+0.14 – -0.12)	(40.37-40.67)	(12.44-10.84)	(47.18-48.49)	(0.341-0.343)
NC-07	(8-14)	(16-21)	(0.292-0.179)	(-6.57 – -6.29)	(+0.10 – -0.03)	(40.42-40.67)	(12.20-10.86)	(47.38-48.47)	(0.341-0.344)
NC-08	(3-8)	(5-7)	(0.311-0.191)	(-7.62 – -7.37)	(-0.05 – -0.23)	(40.31-40.59)	(12.79-11.26)	(46.90-48.14)	(0.343-0.344)
NC-09	(10-14)	(13-15)	(0.306-0.187)	(-7.29 – -7.06)	(-0.15 – -0.31)	(40.35-40.60)	(12.56-11.23)	(47.09-48.17)	(0.345-0.346)
NC-10	(9-13)	(11-14)	(0.309-0.185)	(-7.40 – -7.16)	(-0.11 – -0.30)	(40.32-40.60)	(12.72-11.21)	(46.96-48.18)	(0.345-0.346)
NC-11	(4-8)	(10-11)	(0.288-0.178)	(-6.91 – -6.79)	(+0.05 – -0.10)	(40.40-40.61)	(12.31-11.61)	(47.30-48.23)	(0.341-0.343)
NC-12	(7-10)	(7-9)	(0.293-0.192)	(-8.21 – -7.97)	(-0.51 – -0.61)	(40.12-40.36)	(13.78-12.51))	(46.10-47.13)	(0.348-0.348)
NC-13	(12-16)	(12-14)	(0.314-0.190)	(-7.67 – -7.45)	(-0.27 – -0.42)	(40.30-40.55)	(12.84-11.48)	(46.86-47.96)	(0.347-0.348)
NC-14	(5-10)	(10-13)	(0.302-0.185)	(-7.02 – -6.81)	(+0.04 – -0.14)	(40.36-40.63)	(12.50-11.06)	(47.14-48.31)	(0.342-0.344)
NC-15	(1-6)	(5-7)	(0.313- 0.205)	(-7.77 – -7.48)	(-0.27 – -0.42)	(40.09-40.41)	(13.98-12.25)	(45.94-47.34)	(0.345-0.345)
NC-17	(7-12)	(11-13)	(0.300-0.183)	(-7.27 – -7.06)	(-0.08 – -0.26)	(40.33-40.60)	(12.67-11.24)	(47.00-48.16)	(0.344-0.345)
NC-19	(5-9)	(7-9)	(0.299-0.182)	(-7.59 – -7.34)	(-0.17– -0.34)	(40.29-40.58)	(12.87-11.36)	(46.84-48.07)	(0.344-0.345)
NC-53	(6-10)	(10-12)	(0.311-0.190)	(-7.17 – -6.96)	(+0.06– -0.10)	(40.39-40.62)	(12.37-11.11)	(47.24-48.27)	(0.342-0.343)
NC-54	(7-12)	(11-14)	(0.309-0.185)	(-7.14 – -6.88)	(+0.01– -0.16)	(40.35-40.62)	(12.56-11.10)	(47.09-48.27)	(0.343-0.344)
NC-56	(7-11)	(11-13)	(0.308-0.195)	(-7.14 – -6.77)	(+0.02– -0.10)	(40.34-40.62)	(12.60-11.12)	(47.06-48.26)	(0.343-0.343)

Table (VIIB): Intensive and extensive melting parameters calculating from the composition of the La Conception lavas assuming 4 wt% of their pre-eruptive H_2O content

Parameter	Melting temperatures (T_{Ol-L})				Potential temperatures		Pressure	Melting Fraction	
Reference	Lee et al. (2009)	Beattie (1993)	Putirka et al. (2007)	Putirka (2016)	Putirka (2016)	Putirka (2016)	Lee et al. (2009)	Putirka (2016)	Putirka et al. (2007)
	Tm (ºC)	Tm (ºC)	Tm (ºC)	Tm (ºC)	Tp (ºC)[1]	Tp (ºC)[2]	P(GPa)[1]	Fm %	Fm %*
NC-00	(1183-1199)	(1246-1253)	(1145-1159)	(1166-1173)	(1142-1171)	(1143-1165)	(0.74-0.75)	(<1-1)	(<1-<1)
NC-01	(1175-1197)	(1286-1305)	(1165-1190)	(1206-1225)	(1185-1227)	(1175-1211)	(0.54-0.60)	(1-6)	(2-8)
NC-02	(1178-1194)	(1294-1307)	(1173-1192)	(1214-1227)	(1183-1214)	(1178-1204)	(0.73-0.77)	(<1-2)	(<1-4)
NC-03	(1182-1200)	(1291-1304)	(1174-1194)	(1211-1224)	(1179-1214)	(1176-1205)	((0.79-0.83)	(<1-2)	(<1-4)
NC-04	(1167-1188)	(1272-1286)	(1154-1177)	(1192-1206)	(1162-1201)	(1157-1189)	(0.81-0.86)	(<1-1)	(<1-5)
NC-05	(1181-1194)	(1236-1235)	(1135-1118)	(1157-1155)	(1139-1119)	(1136-1119)	(0.87-0.93)	(<1-<1)	(<1-<1)
NC-06	(1179-1202)	(1292-1310)	(1172)1198)	(1211-1229)	(1168-1204)	(1169-1201)	((0.82-0.87)	(<1-1)	(<1-3)
NC-07	(1191-1215)	(1327-1352)	(1199-1228)	(1246-1271)	(1198-1245)	(1197-1237)	(0.70-0.76)	(<1-5)	(<1-5)
NC-08	(1161-1182)	(1233-1252)	(1129-1154)	(1152-1171)	(1123-1156)	(1125-1154	(0.76-0.81)	(<1-<1)	(<1-<1)
NC-09	(1170-1190)	(1277-1294	(1158-1182)	(1197-1214)	(1164-1203)	(1160-1193)	(0.59-0.64)	(<1-3)	(1-6)
NC-10	(1166-1187)	(1265-1283)	(1150-1175)	(1185-1203)	(1153-1194)	(1151-1185)	(0.56-0.61)	(<1-3)	(<1-6)
NC-11	(1190-1206)	(1284-1294)	(1173-1190)	(1203-1214)	(1166-1192)	(1168-1190)	(0.81-0.84)	(<1-1)	(<1-<1)
NC-12	(1168-1184)	(1205-1221)	(1111-1132)	(1126-1142)	(1114-1147)	(1113-1139)	(0.58-0.62)	(<1-1)	(<1-1)
NC-13	(1154-1173)	(1254-1270)	(1137-1160)	(1175-1191)	(1148-1192)	(1142-1177)	(0.45-0.49)	(<1-3)	(4-9)
NC-14	(1180-1201)	(1283-1300)	(1168-1192)	(1202-1220)	(1163-1198)	(1164-1194)	(0.74-0.79)	(<1-1)	(<1-2)
NC-15	(1178-1201)	(1223-1244)	(1125-1152)	(1143-1164)	(1120-1151)	(1122-1151)	(0.89-0.94)	(<1-<1)	(<1-<1)
NC-17	(1175-1195)	(1270-1287)	(1157-1180)	(1190-1207)	(1158-1195)	(1157-1188)	(0.62-0.67)	(<1-3)	(<1-4)
NC-19	(1170-1191)	(1237-1256)	(1135-1159)	(1157-1176)	(1132-1167)	(1132-1163)	(0.75-0.80)	(<1-<1)	(<1-1)
NC-53	(1170-1190)	(1275-1292)	(1159-1183)	(1194-1212)	(1156-1187)	(1156-1184)	(0.66-0.70)	(<1-<1)	(<1-2)
NC-54	(1173-1196)	(1281-1302)	(1163-1190)	(1201-1221)	(1162-1201)	(1162-1195)	(0.64-0.70)	(<1-2)	(<1-4)
NC-56	(1173-1195)	(1281-1306)	(1163-1192)	(1201-1225)	(1162-1197)	(1162-1194)	(0.64-0.82)	(<1-<1)	(1-2)

Table (VIIB): ***Continued***

Parameter	Melting fraction		Melting redox state			Calculated mantle Olivine Composition			
Reference	Putirka et al. (2007)	Lee & Chin (2014)	Putirka (2016)	Fegley (2013)		Putirka (2016)			
	Fm %**	Fm %	Fe_2O_3/FeO	log fO_2	ΔQFM	SiO2 wt %	FeO_t wt %	MgO wt%	K_D(Fe-Mg)
NC-00	(<1-4)	(9-11)	(0.568-0.301)	(-7.76 - -7.74)	(+0.73-+0.48)	(41.21-40.99)	(7.99—9.17)	(50.80-49.85)	(0.337-0.337)
NC-01	(7-12)	(16-19)	(0.644-0.326)	(-7.37 - -7.18)	(+0.87-+0.64)	(41.35-41.10)	(7.24—8.55)	(51.41-50.34)	(0.341-0.341)
NC-02	(5-8)	(14-16)	(0.635-0.357)	(-7.17 - -7.05)	(+0.93-+0.73)	(41.36-41.13)	(7.19—8.39)	(51.45-50.48)	(0.337-0.338)
NC-03	(4-8)	(13-16)	(0.595-0.315)	(-7.18 - -7.06)	(+0.90-+0.67)	(41.32-41.10)	(7.38—8.55)	(51.30-50.34)	(0.336-0.337)
NC-04	(4-9)	(11-14)	(0.676-0.354)	(-7.40 - -7.29)	(+0.87-+0.60)	(41.37-41.17)	(7.14—8.21)	(51.49-50.62)	(0.338-0.339)
NC-05	(<1-2)	(9-14)	(0.609-0.239)	(-8.13 - -7.93)	(+0.56-+0.52)	(41.22-41.89)	(7.92—9.68)	(50.86-49.43)	(0.340-0.325)
NC-06	(1-7)	(12-15)	(0.667-0.325)	(-7.11 - -6.96)	(+1.02-+0.79)	(41.35-41.13)	(7.21—8.43)	(51.44-50.44)	(0.335-0.337)
NC-07	(4-10)	(17-22)	(0.604-0.315)	(-6.77 - -6.53)	(+1.13-+0.89)	(41.35-41.14)	(7.26—8.36)	(51.39-50.50)	(0.336-0.337)
NC-08	(<1-4)	(6-9)	(0.663-0.340)	(-7.81 - -7.63)	(+0.88-+0.68)	(41.32-41.09)	(7.40—8.60)	(51.28-50.30)	(0.337-0.337)
NC-09	(6-10)	(13-16)	(0.658-0.337)	(-7.43 - -7.26)	(+0.95-+0.72)	(41.37-41.12)	(7.14—8.44)	(51.49-50.44)	(0.340-0.340)
NC-10	(5-9)	(12-15)	(0.667-0.332)	(-7.55 - -7.38)	(+0.96-+0.71)	(41.35-41.12)	(7.21—8.49)	(51.44-50.40)	(0.339-0.340)
NC-11	(<1-5)	(11-13)	(0.577-0.305)	(-7.23 - -7.15)	(+0.92-+0.74)	(41.29-41.06)	(7.56—8.80)	(51.15-50.14)	(0.335-0.336)
NC-12	(3-6)	(8-10)	(0.621-0.351)	(-8.36- -8.19)	(+0.60-+0.41)	(41.24-41.01)	(7.84—9.03)	(50.49-49.96)	(0.342-0.341)
NC-13	(8-12)	(12-15)	(0.694-0.350)	(-7.76 - -7.60)	(+0.93-+0.65)	(41.37-41.11)	(7.11—8.51)	(51.51-50.38)	(0.342-0.342)
NC-14	(1-7)	(11-15)	(0.630-0.324)	(-7.24 - -7.09)	(+1.00-+0.78)	(41.33-41.11)	(7.33—8.49)	(51.34-50.39)	(0.336-0.337)
NC-15	(<1-2)	(6-9)	(0.732-0.370)	(-7.99 - -7.78)	(+0.66-+0.49)	(41.31-41.06)	(7.43—8.78)	(51.25-50.16)	(0.338-0.338)
NC-17	(4-8)	(12-15)	(0.633-0.324)	(-7.46 - -7.32)	(+0.94-+0.70)	(41.33-41.10)	(7.36—8.57)	(51.31-50.33)	(0.338-0.339)
NC-19	(1-5)	(8-11)	(0.621-0.318)	(-7.84 - -7.66)	(+0.77-+0.56)	(41.28-41.05)	(7.63—8.82)	(51.09-50.13)	(0.338-0.338)
NC-53	(2-6)	(10-13)	(0.667-0.341)	(-7.33 - -7.17)	(+1.05-+0.87)	(41.38-41.13)	(7.05—8.39)	(51.56-50.48)	(0.336-0.337)
NC-54	(3-8)	(12-15)	(0.661-0.331)	(-7.30 - -7.10)	(+1.04-+0.81)	(41.36-41.13)	(7.16—8.43)	(51.47-50.44)	(0.337-0.338)
NC-56	(3-7)	(12-16)	(0.658-0.349)	(-7.30 - -7.01)	(+1.04-+0.85)	(41.36-41.13)	(7.20—8.39)	(51.44-50.48)	(0.337-0.337)

Table (VIIC): Intensive and extensive melting parameters calculating from the composition of the La Conception lavas assuming 8 wt% of their pre-eruptive H_2O content

Parameter	Melting temperatures (TOl-L)				Potential temperatures		Pressure	Melting Fraction	
Reference	Lee et al. (2009)	Beattie (1993)	Putirka et al. (2007)	Putirka (2016)	Putirka et al. (2007)	Putirka. (2016)	Lee et al. (2009)	Putirka (2016)	Putirka et al. (2007)
	Tm (ºC)	Tm (ºC)	Tm (ºC)	Fm %	Fm %*	Tp (ºC)[2]	P (GPa)[1]	Fm %	Fm %*
NC-00	(1137-1148)	(1236-1239)	(1061-1070)	(1076-1079)	(1060-1072)	(1060-1071)	(0.91-0.93)	(<1-<1)	(<1-<1)
NC-01	(1127-1141)	(1280-1297)	(1084-1104)	(1121-1138)	(1090-1126)	(1086-1115)	(0.71-0.76)	(<1-<1)	(<1-3)
NC-02	(1132-1143)	(1287-1297)	(1090-1104)	(1127-1137)	(1087-1114)	(1088-1108)	(0.88-0.92)	(<1-<1)	(<1-<1)
NC-03	(1136-1148)	(1282-1292)	(1090-1104)	(1122-1133)	(1085-1113)	(1087-1108)	(0.94-0.97)	(<1-<1)	(<1-<1)
NC-04	(1128-1142)	(1266-1277)	(1075-1091)	(1106-1117)	(1070-1103)	(1072-1096)	(0.96-1.00)	(<1-<1)	(<1-1)
NC-05	(1139-1144)	(1228-1207)	(1054-1018)	(1068-1047)	(1053-1026)	(1053-1023)	(1.02-1.09)	(<1-<1)	(<1-<1)
NC-06	(1135-1150)	(1284-1298)	(1090-1109)	(1123-1138)	(1084-1109)	(1086-1108)	(0.97-1.01)	(<1-<1)	(<1-<1)
NC-07	(1139-1155)	(1320-1341)	(1114-1137)	(1160-1181)	(1108-1141)	(1110-1138)	(0.85-0.91)	(<1-<1)	(<1-<1)
NC-08	(1124-1138)	(1226-1242)	(1053-1071)	(1067-1082)	(1048-1068)	(1050-1069)	(0.93-0.97)	(<1-<1)	(<1-<1)
NC-09	(1125-1138)	(1272-1286)	(1079-1097)	(1112-1127)	(1078-1104)	(1078-1100)	(0.75-0.80)	(<1-<1)	(<1-2)
NC-10	(1122-1136)	(1260-1275)	(1071-1090)	(1100-1115)	(1068-1096)	(1069-1093)	(0.73-0.78)	(<1-<1)	(<1-1)
NC-11	(1141-1152)	(1272-1280)	(1087-1099)	(1112-1120)	(1082-1097)	(1084-1097)	(0.97-1.00)	(<1-<1)	(<1-<1)
NC-12	(1125-1137)	(1200-1214)	(1036-1051)	(1041-1054)	(1037-1054)	(1037-1054)	(0.77-0.81)	(<1-<1)	(<1-<1)
NC-13	(1113-1125)	(1251-1265)	(1061-1079)	(1092-1105)	(1065-1090)	(1062-1084)	(0.63-0.67)	(<1-<1)	(<1-<1)
NC-14	(1134-1148)	(1275-1289)	(1086-1103)	(1115-1129)	(1081-1103)	(1082-1103)	(0.90-0.94)	(<1-<1)	(<1-4)
NC-15	(1138-1154)	(1216-1233)	(1048-1067)	(1057-1074)	(1045-1066)	(1046-1066)	(1.05-1.10)	(<1-<1)	(<1-<1)
NC-17	(1128-1142)	(1264-1276)	(1076-1093)	(1104-1117)	(1073-1098)	(1074-1095)	(0.79-0.84)	(<1-<1)	(<1-<1)
NC-19	(1129-1144)	(1229-1244)	(1055-1073)	(1069-1085)	(1052-1073)	(1053-1073)	(0.92-0.97)	(<1-<1)	(<1-<1)
NC-53	(1126-1139)	(1269-1284)	(1080-1098)	(1109-1124)	(1075-1097)	(1077-1097)	(0.82-0.86)	(<1-<1)	(<1-<1)
NC-54	(1127-1142)	(1275-1293)	(1083-1104)	(1116-1133)	(1078-1106)	(1080-1104)	(0.80-0.85)	(<1-<1)	(<1-<1)
NC-56	(1127-1145)	(1275-1297)	(1083-1106)	(1116-1137)	(1078-1105)	(1080-1105)	(0.81-0.96)	(<1-<1)	(<1-<1)

-

Table (VIIC): ***Continued***

Parameter	Melting fraction		Melting redox state			Calculated mantle Olivine Composition			
Reference	Putirka et al. (2007)	Lee & Chin (2014)	Putirka (2016)	Fegley (2013)		Putirka (2016)			
	Fm %**	Fm %	Fe_2O_3/FeO	log fO_2	ΔQFM	SiO_2 wt %	FeO_t wt %	MgO wt%	K_D(Fe-Mg)
NC-00	(<1-<1)	(11-13)	(0.827-0.443)	(-8.05 - -8.05)	(+1.41-+1.20)	(41.49-41.23)	(6.46-7.86)	(52.04-50.90)	(0.331-0.330)
NC-01	(3-7)	(16-20)	(0.926-0.482)	(-7.48 - -7.34)	(+1.73-+1.47)	(41.64-41.35)	(5.71-7.21)	(52.66-51.43)	(0.335-0.335)
NC-02	(<1-4)	(15-18)	(0.934-0.521)	(-7.33 - -7.26)	(+1.75-+1.53)	(41.63-41.38)	(5.73-7.06)	(52.64-51.56)	(0.331-0.332)
NC-03	(<1-4)	(14-17)	(0.869 -0.456)	(-7.37 - -7.31)	(+1.69-+1.44)	(41.59-41.34)	(5.93-7.30)	(52.47-51.36)	(0.330-0.331)
NC-04	(<1-4)	(12-15)	(0.998 -0.517)	(-7.53 - -7.49)	(+1.69-+1.40)	(41.65-41.41)	(5.65-6.91)	(52.71-51.68)	(0.333-0.333)
NC-05	(<1-<1)	(11-17)	(0.894 -0.332)	(-8.13 - -8.77)	(+1.31-+1.03)	(41.52-41.11)	(5.33-8.53)	(52.15-51.36)	(0.340-0.316)
NC-06	(<1-3)	(13-17)	(0.973 -0.469)	(-7.29 - -7.21)	(+1.75-+1.52)	(41.63-41.36)	(5.74-7.18)	(52.63-51.46)	(0.329-0.330)
NC-07	(<0-6)	(18-24)	(0.887 -0.459)	(-6.92 – 6.74)	(+1.90-+1.70)	(41.62-41.37)	(5.81-7.12)	(52.57-51.51)	(0.331-0.331)
NC-08	(<1-<1)	(6-10)	(0.971 -0.494)	(-7.95 - -7.85)	(+1.59-+1.40)	(41.60-41.34)	(5.88-7.29)	(52.51-51.37)	(0.334-0.334)
NC-09	(2-6)	(14-17)	(0.979 -0.498)	(-7.54 - -7.43)	(+1.75-+1.55)	(41.65-41.37)	(5.63-7.10)	(52.72-51.52)	(0.333-0.334)
NC-10	(<1-5)	(12-16)	(0.990 -0.489)	(-7.66 - -7.56)	(+1.75-+1.52)	(41.64-41.36)	(5.68-7.16)	(52.68-51.47)	(0.328-0.329)
NC-11	(<1-1)	(13-15)	(0.833 -0.436)	(-7.47 - -7.45)	(+1.60-+1.43)	(41.56-41.29)	(6.13-7.56)	(52.31-51.15)	(0.336-0.335)
NC-12	(<1-1)	(8-11)	(0.926 -0.519)	(-8.48 - -8.37)	(+1.90-+1.73)	(41.54-41.29)	(6.21-7.57)	(52.25-51.15)	(0.336-0.336)
NC-13	(3-7)	(13-16)	(1.043 -0.522)	(-7.82 - -7.72)	(+1.76-+1.55)	(41.67-41.37)	(5.55-7.11)	(52.79-51.52)	(0.330-0.331)
NC-14	(<1-2)	(12-16)	(0.921 -0.470)	(-7.41 - -7.32)	(+1.72-+1.52)	(41.61-41.35)	(5.86-7.23)	(52.64-51.42)	(0.332-0.331)
NC-15	(<1-<1)	(7-10)	(1.074 -0.536)	(-8.14 - -8.02)	(+1.37-+1.18)	(41.61-41.32)	(5.85-7.39)	(52.54-51.29)	(0.338-0.338)
NC-17	(<1-4)	(13-16)	(0.993- 0.473)	(-7.61 - -7.54)	(+1.70-+1.48)	(41.61-41.34)	(5.85-7.27)	(52.54-51.39)	(0.332-0.332)
NC-19	(<1-1)	(9-12)	(0.908- 0.460)	(-8.03 - -7.93)	(+1.48-+1.28)	(41.56-41.30)	(6.11-7.52)	(52.33-51.18)	(0.331-0.331)
NC-53	(<1-2)	(11-14)	(0.983- 0.499)	(-7.46 - -7.35)	(+1.80-+1.62)	(41.66-41.38)	(5.58-7.08)	(52.76-51.54)	(0.331-0.331)
NC-54	(0-4)	(13-17)	(0.978- 0.484)	(-7.42 - -7.29)	(+1.81-+1.59)	(41.64-41.37)	(5.67-7.13)	(52.69-51.50)	(0.332-0.332)
NC-56	(0-2)	(13-16)	(0.973- 0.509)	(-7.42 - -7.20)	(+1.81-+1.60)	(41.64-41.38)	(5.70-7.08)	(52.66-51.54)	(0.332-0.331)

References

Ariskin, A.A. and Nikolaev, G.S. (1996) An empirical model for the calculation of spinel?melt equilibria in mafic igneous systems at atmospheric pressure: 1. Chromian spinels. ***Contributions to Mineralogy and Petrology*** 123, 282–292.

Asimov, P.D.; Hirschmann, M.M. and Stolper, E.M. (1997) An analysis of variations in isentropic melt productivity. ***Philosophical Transactions of the Royal Society of London, Sries A,***355, 255-281.

Beattie, P. (1993) Olivine-melt and orthopyroxene-melt equilibria. ***Contributions to Mineralogy and Petrology***115, 103–111.

Borisov, A.A. and Shapkin, A.I. (1990) A new empirical equation rating Fe^{3+}/Fe^{2+} in magmas to their composition, oxygen fugacity, and temperature. ***Geochemistry International*** 27, 111–116.

Bottinga, Y. and Weill, D.F. (1972) The viscosity of magmatic silicate liquids: A model for calculation. ***American Journal of Science*** 272, 438–475.

Dunn, T. and Sen, C. (1994). Mineral/Matrix Partition-Coefficients for Ortho-Pyroxene, Plagioclase, and Olivine in Basaltic to Andesitic Systems - a Combined Analytical and Experimental-Study. ***Geochimica et Cosmochimica Acta*** 58, 717-733.

Fegley, B. Jr. (2013) Practical chemical thermodynamics for geoscientists. Academic Press, New York.

Gale, A.; Dalton, C.A.; Langmuir, C. H.; Su, Y. and Schilling, J.-G. (2013) The mean composition of ocean ridge basalts. ***Geochemistry, Geophysics, Geosystem*** 14. doi:10.1029/2002GC000427.

Hart, S. R. and Dunn, T. (1993) Experimental cpx/melt partitioning of 24 trace elements. ***Contributions to Mineralogy and Petrology*** 113, 1-8.

Horn, I.; Foley, S.F.; Jackson, S.E. and Jenner, G.A. (1994) Experimentally determined partitioning of high field strength- and selected transition elements between spinel and basaltic melt. ***Chemical Geology*** 117 193-218.

Ionov, D. A.; Bodinier, J.-L.; Mukasa, S.B. and Zanetti, A. (2002). Mechanisms and sources of mantle metasomatism: major and trace element compositions of peridotite xenoliths from Spitsbergen in the context of numerical modeling. ***Journal of Petrology*** 43, 2219–2259.

Iwamori, H.; Mc Kenzie, D. and Takahashi, E. (1995) Melt generation by isentropic mantle upwelling. ***Earth and Planetary Science Letters*** 134, 253-266.

Johnson, K.T.M. (1998) Experimental determination of partition coefficients for rare earth and high-field-strength elements between clinopyroxene, garnet, and basaltic melt at high pressures. ***Contributions to Mineralogy and Petrology*** 133, 60-68.

Johnson, K.T. M.; Dick, H.J.B. and Shimizu, N. (1990) Melting in the oceanic upper mantle: An ion microprobe study of diopsides in Abyssal peridotites. ***Journal of Geophysical Research*** 95, 2661-2678.

Kelemen P.B.; Shimizu, N.; Dunn, T. (1993) Relative depletion of niobium in some arc magmas and the continental crust: partitioning of K, Nb, La, and Ce during melt/rock reaction in the upper mantle. ***Earth and Planetary Science Letters*** 120, 111-134.

Kennedy, A.K; Lofgren G.E. and Wasserburg, G.J. (1993) An experimental study of trace element partitioning between olivine, orthopyroxene and melt in chondrules: equilibrium values and kinetic effects. ***Earth and Planetary Science Letters*** 115,177-195.

Lange, R. A. and Carmichael, I. S. E. (1987), Densities of Na_2O-K_2O-CaO-MgO-FeO-Fe_2O_3-Al_2O_3-TiO_2-SiO_2 liquids: New measurements and derived partial molar properties. ***Geochimica et Cosmochimica Acta*** 51, 2931-2946.

Laubier, M., Grove, T.L., Langmuir, C.H. (2014) Trace element mineral/melt partitioning for basaltic and basaltic andesitic melts: an experimental and laser ICP-MS study with application to the oxidation state of mantle source regions. ***Earth Planet. Sci. Lett.*** 392, 265–278.

Lee, C-T., and Chin, E.J. (2014) Calculating melting temperatures and pressure of peridotite protoliths: Implications for the origin of cratonic mantle. ***Earth and Planetary Science Letters*** 403, 273–286.

Lee, C.-T. A.; Luffi, P.; Plank, T.; Dalton, H. and Leeman; W.P. (2009), Constraints on the depths and temperatures of basaltic magma generation on earth and other terrestrial planets using new thermobarometers for mafic magmas. ***Earth and Planetary Science Letters***279, 20–33.

McDonough, W. F. and Sun, S.-S. (1995) The composition of the Earth. ***Chemical Geology*** 120, 223–253.

Nicholson, K.N.; Maurizot, P.P.; Black, P.M., Picard, C.; Simonetti, A.A., Stewart, A. and Alexander, A.A. (2011) Geochemistry and age of the Noumea Basin lavas,

New Caledonia; evidence for Cretaceous subduction beneath the eastern Gondwana margin. ***Lithos*** 125, 659-674.

Nielsen, R.L., Gallahan, W.E. and Newberger, F. (1992). Experimentally determined mineral-melt partition coefficients for Sc, Y and REE for olivine, orthopyroxene, pigeonite, magnetite and ilmenite. ***Contributions to Mineralogy and Petrology*** 110, 488-499.

Putirka, K. (2016) Rates and styles of planetary cooling on Earth, Moon, Mars, and Vesta, using new models for oxygen fugacity, ferric-ferrous ratios, olivine-liquid Fe-Mg exchange, and mantle potential temperature. ***American Mineralogist*** 101, 819-840.

Putirka, K.; Perfit, M.; Ryerson, F.J. and Jackson, M.G. (2007) Ambient and excess mantle temperatures, olivine thermometry, and active vs. passive upwelling. ***Chemical Geology*** 241,177-206.

Righter, K.; Leeman, W.P. and Hervig, R.L. (2006) Partitioning of Ni, Co and V between spinel structured oxides and silicate melts: Importance of spinel composition. ***Chemical Geology*** 227, 1- 25.

Shaw, D.M. (1970) Trace element fractionation during anatexis. ***Geochimica et Cosmochimica Acta*** 34 237–243.

Takazawa, E. Frey, F.A., Shimizu, N. and Obata, M. (2000) Whole rock compositional variations in an upper mantle peridotite (Horoman, Hokkaido, Japan): Are they consistent with a partial melting process? ***Geochimica et Cosmochimica Acta*** 64, 4, 695–716

Walter, M.J. (1998) Melting of garnet peridotite and the origin of komatiite and depleted lithosphere. ***Journal of Petrology*** 39, 29-60.

Walter, M.J. (1999) Comments on 'Mantle Melting and Melt Extraction Processes beneath Ocean Ridges Evidence from Abyssal Peridotites' by Yaoling Niu. ***Journal of Petrology*** 40, 1187-1193.

Weaver, J. S., and Langmuir, C. H. (1990) Calculation of phase equilibrium in mineral-melt systems. ***Computers & Geosciences*** 16, 1-19.

Wijbrans, C. H.; · Klemme S.; Berndt, J. and Vollmer, C. (2015) Experimental determination of trace element partition coefficients between spinel and silicate melt: the influence of chemical composition and oxygen fugacity. ***Contrib Mineral Petrol*** 1691, 45-77.

Yang, H.-J.; Sen, G. and Shimizu, N. (1998) Mid-ocean ridge melting: constraints from lithospheric xenoliths at Oahu, Hawaii. ***Journal of Petrology*** 39, 277-295.

Zack, T., Foley, S.F. and Jenner, G.A. (1997) A consistent partition coeddicient set for clinopyroxene, amphibole and garnet from laser ablation microprobe analysis of garnet pyrocenites fron Kakanui, New Zealand. ***Neues Jahrbuch für Mineralogie Abhandlungen*** 172, 23-41**.**

.